

**Table 2 Selectivities of metalloprotease inhibitors**

	MMP3	ADAM9	ADAM10	ADAM12	ADAM17
GM6001 (refs. 20,21) <sup>a</sup>	27	n.d.	110	>10,000	1.3
KB-R7785 (refs. 22,23)	3.0	n.d.	n.d.	<1 <sup>b</sup>	9.6
INCB3619 (ref. 24)	3,560	>5,000	22	n.d.	14
INCB4298 (ref. 24)	3,179	1,000	>5,000	n.d.	<5
INCB8765 (ref. 24)	>5,000	>5,000	97	n.d.	2,045

ADAM, a disintegrin and metalloproteinase; MMP, matrix metalloproteinase.  
<sup>a</sup>The values of GM6001 are expressed in Ki (nmol/l). The values of other inhibitors are expressed in 50% inhibitory concentrations (IC<sub>50</sub>, nmol/l). n.d., not determined (20–24). <sup>b</sup>Estimated values from other data (22,23).

respectively ( $P < 0.01$ ), but not with INCB8765, an ADAM10-selective inhibitor (Figure 3c).

#### Effect of recombinant HB-EGF on HB-EGF shedding in 3T3-L1 adipocytes

HB-EGF may play a role in wound healing, tumor growth, and cardiovascular diseases via endocrine, paracrine, and/or autocrine mechanisms (9,10). In this study, HB-EGF mRNA expression is increased only in the adipose tissue from obese animals (see **Supplementary Figure S2a** online). It is, therefore, likely that HB-EGF, when proteolytically released, induces HB-EGF shedding in adipocytes in an autocrine manner. Treatment with recombinant HB-EGF resulted in a time- and dose-dependent increase in HB-EGF shedding in 3T3-L1/HB-EGF-AP adipocytes (Figure 4a,b). Recombinant HB-EGF also induced an ~1.5-fold increase in HB-EGF mRNA expression in 3T3-L1 adipocytes (Figure 4c). In this study, we used recombinant HB-EGF at a dose of 50 ng/ml, because Hashimoto *et al.* showed with HB-EGF at doses of 10–20 ng/ml that HB-EGF acts as a growth factor in human keratinocytes (25). The HB-EGF-induced HB-EGF shedding was significantly suppressed by U0126 and PD98059 ( $P < 0.01$ ) (see **Supplementary Figure S5** online), but was not suppressed by LY294002 (data not shown). Importantly, HB-EGF-induced HB-EGF shedding was significantly inhibited by treatment with both GM6001 and KB-R7785 relative to vehicle-treated groups ( $P < 0.01$ ) (Figure 4d). Furthermore, HB-EGF-induced HB-EGF shedding was markedly suppressed by INCB3619 and INCB4298 ( $P < 0.01$ ) and, to a lesser extent, by INCB8765 ( $P < 0.01$ ) (Figure 4e). The insulin-induced HB-EGF shedding was significantly inhibited by treatment with AG1478 ( $P < 0.01$ ) (Figure 3d).

#### Effect of HB-EGF on metabolic phenotypes in 3T3-L1 adipocytes

HB-EGF treatment (50 ng/ml) either for 1 h or 24 h did not affect insulin-induced glucose uptake (see **Supplementary Figure S6a** online). Triglyceride contents in 3T3-L1 adipocytes were unaltered by HB-EGF treatment for 48 h (see **Supplementary**

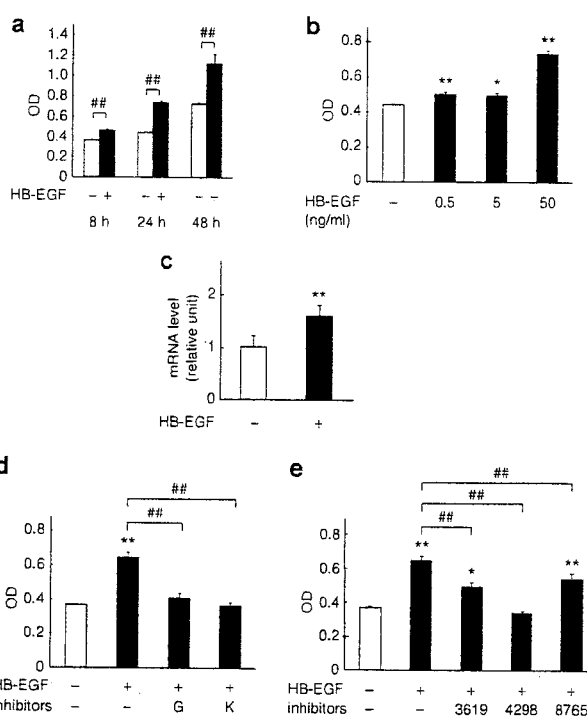


**Figure 4** Effect of recombinant HB-EGF on HB-EGF shedding and mRNA expression in 3T3-L1 adipocytes. (a) Time course of HB-EGF shedding in differentiated 3T3-L1/HB-EGF-AP adipocytes treated with recombinant HB-EGF. Optical density (OD) shows the absorbance at 405 nm, which indicates AP activity in the conditioned media. Open bars, vehicle; filled bars, recombinant HB-EGF (50 ng/ml). (b) Dose response of HB-EGF shedding in 3T3-L1/HB-EGF-AP adipocytes treated with recombinant HB-EGF for 24 h. Open bar, vehicle; filled bars, recombinant HB-EGF with indicated doses. (c) HB-EGF mRNA expression in 3T3-L1 adipocytes treated with recombinant HB-EGF for 24 h. Open bar, vehicle; filled bar, recombinant HB-EGF (50 ng/ml). (d) Effect of broad metalloprotease inhibitors on HB-EGF shedding in 3T3-L1/HB-EGF-AP adipocytes treated with recombinant HB-EGF for 24 h. Open bar, vehicle; filled bars, recombinant HB-EGF (50 ng/ml) with or without inhibitors. G, GM6001 (20  $\mu$ mol/l); K, KB-R7785 (10  $\mu$ mol/l). (e) Effect of ADAM-selective inhibitors on HB-EGF shedding in 3T3-L1/HB-EGF-AP adipocytes treated with recombinant HB-EGF for 24 h. Open bar, vehicle; filled bars, recombinant HB-EGF (50 ng/ml) with or without inhibitors. 3,619, INCB3619 (1  $\mu$ mol/l); 4298, INCB4298 (1  $\mu$ mol/l); 8765, INCB8765 (1  $\mu$ mol/l). \* $P < 0.05$ , \*\* $P < 0.01$  vs. vehicle. \*\* $P < 0.01$ .  $n = 6$ . AP, alkaline phosphatase; HB-EGF, heparin-binding epidermal growth factor-like growth factor; n.s., not significant; 3T3-L1/HB-EGF-AP, 3T3-L1 with stable expression of AP-tagged proHB-EGF.

**Figure S6b** online). On the other hand, mRNA expression of monocyte chemoattractant protein-1, a major chemokine implicated in macrophage infiltration (1), was increased by HB-EGF treatment for 24 h (see **Supplementary Figure S6c** online), suggesting the pathophysiological role of HB-EGF.

#### DISCUSSION

There are numerous proteolytic enzymes expressed in adipocytes *in vitro* or in the adipose tissue *in vivo* (7,8), suggesting that proteolytic cleavage and release of membrane proteins is a crucial regulatory step for some adipocytokines. HB-EGF, which is expressed in the adipose tissue (12), is a prototypic

transmembrane protein that is proteolytically cleaved to release a soluble form via members of the ADAM family of proteolytic enzymes (10). A previous report showed that plasma concentrations of HB-EGF are elevated in proportion to the degree of adiposity in humans or in obese patients with coronary artery disease, suggesting the pathophysiologic role of HB-EGF as an adipocytokine (12). It is, therefore, important to know the regulatory mechanism of HB-EGF shedding in adipocytes.

Using 3T3-L1/HB-EGF-AP adipocytes which we have developed, we demonstrated that insulin induces a time- and dose-dependent increase in HB-EGF shedding in differentiated 3T3-L1 adipocytes. Importantly, insulin-induced HB-EGF shedding in adipocytes is suppressed by pharmacologic blockade of ADAM17, suggesting the role of ADAM17 in insulin-induced HB-EGF shedding in adipocytes. In this study, insulin is capable of inducing HB-EGF shedding in adipocytes as long as 48 h after the treatment. Because insulin induces the cleavage and release of the extracellular domain of Klotho in COS-7 cells within 1–2 h (26), insulin may indirectly activate ADAM17 to induce HB-EGF shedding in adipocytes. In this regard, Tanida *et al.* previously reported that interleukin-1 $\beta$  can upregulate the secretion of interleukin-8, which in turn activates ADAM10 to induce HB-EGF shedding in KATO-III cells, a human gastric cancer cell line (27). It is interesting to speculate that insulin activates ADAM17 to induce HB-EGF shedding in 3T3-L1 adipocytes via an indirect mechanism.

Given that insulin-induced HB-EGF shedding is effectively suppressed by treatment with mitogen-activated protein kinase/extracellular signal-regulated kinase inhibitors, it is conceivable that insulin-induced HB-EGF shedding in adipocytes is mediated at least in part by an adipocyte-derived factor in a mitogen-activated protein kinase-dependent manner. On the other hand, insulin-induced HB-EGF shedding in 3T3-L1/HB-EGF-AP adipocytes was not suppressed and rather increased by a phosphoinositide 3-kinase inhibitor. Although the mechanism by which insulin-induced HB-EGF shedding is increased by phosphoinositide 3-kinase inhibition is unknown, it is likely that insulin induces HB-EGF shedding in adipocytes via a pathway different from that in insulin-induced shedding of Klotho or syndecan (26,28).

In this study, there is no significant induction of HB-EGF shedding in undifferentiated 3T3-L1 preadipocytes treated with insulin. By contrast, phorbol 12-myristate 13-acetate induces HB-EGF shedding in both undifferentiated 3T3-L1 preadipocytes and differentiated 3T3-L1 adipocytes, which is suppressed by an ADAM17-selective inhibitor INCB4298 (data not shown). In this regard, a previous study reported that preadipocyte factor 1, an EGF repeat containing transmembrane protein, can be cleaved in undifferentiated 3T3-L1 preadipocytes via ADAM17 *in vitro* (29), suggesting that ADAM17 is functional even in undifferentiated 3T3-L1 preadipocytes. Further studies are required to elucidate how insulin regulates differentially HB-EGF shedding in undifferentiated 3T3-L1 preadipocytes and differentiated 3T3-L1 adipocytes.

Regulated shedding of cell surface proteins should be a mechanism for activation of autocrine and paracrine signaling

in a variety of cell types (30). Our data revealed that HB-EGF mRNA is expressed in the stromal-vascular fraction, as well as in the adipocyte fraction, from rodent model of obesity. Because HB-EGF is reported to be produced in macrophage-like cells (9), it is likely that HB-EGF shedding in obese adipose tissue is activated by macrophages in a paracrine manner. On the other hand, treatment with AG1478 inhibited insulin-induced HB-EGF shedding, suggesting that adipocyte-derived EGF receptor ligands including HB-EGF can activate insulin-induced HB-EGF shedding in 3T3-L1 adipocytes *in vitro*. Further studies are required to elucidate the detailed mechanism of insulin-induced HB-EGF shedding in adipocytes.

Proteolytic cleavage and release of membrane proteins in adipocytes may represent an attractive therapeutic target for the treatment and prevention of the metabolic syndrome. For instance, mice heterozygous for ADAM17 have been protected from obesity-induced insulin resistance and diabetes (31). Furthermore, mice lacking the Zn<sup>2+</sup> binding region of the catalytic domain of ADAM17, have exhibited decrease in body weight and fat mass relative to wild-type mice (32). On the other hand, mice lacking TNF $\alpha$ , those lacking the TNF $\alpha$  receptor p55 subunit, and those lacking both p55 and p75 have been all protected from obesity-induced insulin resistance but not from obesity (33–35). It is interesting to speculate that besides TNF $\alpha$ , membrane protein(s) which undergo proteolytic cleavage by ADAM17 play a role in the development of obesity. Given that EGF receptor signaling is involved in adipogenesis *in vitro* and obesity-related phenotypes *in vivo* (36,37), HB-EGF may be one of such adipocytokines that can modulate locally adipogenesis and obesity.

Our data revealed that HB-EGF mRNA expression is high in the adipose tissue from rodent models of obesity. In addition, HB-EGF mRNA is increased only in the adipose tissue. On the other hand, serum HB-EGF levels are higher in obese human subjects relative to lean normal control subjects (12). It is, therefore, conceivable that the elevated serum HB-EGF in obese subjects is derived from the adipose tissue. It is reported that HB-EGF can stimulate the proliferation and migration of bovine aortic smooth muscle cells *in vitro* (38) and the formation of atherosclerotic plaques *in vivo* (39). These findings, taken together, suggest that HB-EGF, which is derived from the adipose tissue, is involved in obesity-related cardiovascular diseases.

In conclusion, this study provides *in vitro* evidence that insulin induces HB-EGF shedding in 3T3-L1 adipocytes. Our data also suggest the role of ADAM17 in insulin-induced HB-EGF shedding in adipocytes. Further studies are required to elucidate the detailed mechanism of insulin-induced HB-EGF shedding in adipocytes.

#### SUPPLEMENTARY MATERIAL

Supplementary material is linked to the online version of the paper at <http://www.nature.com/oby>

#### ACKNOWLEDGMENTS

We thank Dr Kitamura for Plat-E and Dr Yamaoka for pMRX-IRES-Puro vector. This work was supported in part by a Grant-in-Aid for Scientific

Research from the Ministry of Education, Culture, Sports, Science, and Technology of Japan, and Ministry of Health, Labor, and Welfare of Japan, and research grants from Takeda Science Foundation.

#### DISCLOSURE

The authors declared no conflict of interest.

© 2010 The Obesity Society

#### REFERENCES

- Matsuzawa Y, Funahashi T, Nakamura T. Molecular mechanism of metabolic syndrome X: contribution of adipocytokines adipocyte-derived bioactive substances. *Ann N Y Acad Sci* 1999;892:146–154.
- Lyon CJ, Law RE, Hsueh WA. Minireview: adiposity, inflammation, and atherogenesis. *Endocrinology* 2003;144:2195–2200.
- Suganami T, Nishida J, Ogawa Y. A paracrine loop between adipocytes and macrophages aggravates inflammatory changes: role of free fatty acids and tumor necrosis factor  $\alpha$ . *Arterioscler Thromb Vasc Biol* 2005;25:2062–2068.
- Suganami T, Tanimoto-Koyama K, Nishida J *et al*. Role of the Toll-like receptor 4/NF- $\kappa$ B pathway in saturated fatty acid-induced inflammatory changes in the interaction between adipocytes and macrophages. *Arterioscler Thromb Vasc Biol* 2007;27:84–91.
- Burgess TL, Kelly RB. Constitutive and regulated secretion of proteins. *Annu Rev Cell Biol* 1987;3:243–293.
- Bradley RL, Cleveland KA, Cheatham B. The adipocyte as a secretory organ: mechanisms of vesicle transport and secretory pathways. *Recent Prog Horm Res* 2001;56:329–358.
- Chavey C, Mari B, Monthouel MN *et al*. Matrix metalloproteinases are differentially expressed in adipose tissue during obesity and modulate adipocyte differentiation. *J Biol Chem* 2003;278:11888–11896.
- Seals DF, Courtneidge SA. The ADAMs family of metalloproteinases: multidomain proteins with multiple functions. *Genes Dev* 2003;17:7–30.
- Higashiyama S, Abraham JA, Miller J, Fiddes JC, Klagsbrun M. A heparin-binding growth factor secreted by macrophage-like cells that is related to EGF. *Science* 1991;251:936–939.
- Higashiyama S, Nanba D. ADAM-mediated ectodomain shedding of HB-EGF in receptor cross-talk. *Biochim Biophys Acta* 2005;1751:110–117.
- Yamada A, Kawata S, Tamura S *et al*. Plasma heparin-binding EGF-like growth factor levels in patients after partial hepatectomy as determined with an enzyme-linked immunosorbent assay. *Biochem Biophys Res Commun* 1998;246:783–787.
- Matsumoto S, Kishida K, Shimomura I *et al*. Increased plasma HB-EGF associated with obesity and coronary artery disease. *Biochem Biophys Res Commun* 2002;292:781–786.
- Ito A, Suganami T, Miyamoto Y *et al*. Role of MAPK phosphatase-1 in the induction of monocyte chemoattractant protein-1 during the course of adipocyte hypertrophy. *J Biol Chem* 2007;282:25445–25452.
- Tokumaru S, Higashiyama S, Endo T *et al*. Ectodomain shedding of epidermal growth factor receptor ligands is required for keratinocyte migration in cutaneous wound healing. *J Cell Biol* 2000;151:209–220.
- Saitoh T, Nakayama M, Nakano H *et al*. TWEAK induces NF- $\kappa$ B2 p100 processing and long lasting NF- $\kappa$ B activation. *J Biol Chem* 2003;278:36005–36012.
- Morita S, Kojima T, Kitamura T. Plat-E: an efficient and stable system for transient packaging of retroviruses. *Gene Ther* 2000;7:1063–1066.
- Goishi K, Higashiyama S, Klagsbrun M *et al*. Phorbol ester induces the rapid processing of cell surface heparin-binding EGF-like growth factor: conversion from juxtacrine to paracrine growth factor activity. *Mol Biol Cell* 1995;6:967–980.
- Huovila AP, Turner AJ, Pelto-Huikko M, Kärkkäinen I, Ortiz RM. Shedding light on ADAM metalloproteinases. *Trends Biochem Sci* 2005;30:413–422.
- Folgueras AR, Pendás AM, Sánchez LM, López-Otín C. Matrix metalloproteinases in cancer: from new functions to improved inhibition strategies. *Int J Dev Biol* 2004;48:411–424.
- Galardy RE, Grobelny D, Foellmer HG, Fernandez LA. Inhibition of angiogenesis by the matrix metalloproteinase inhibitor N-[2R-2-(hydroxamidocarbonylmethyl)-4-methylpentanoyl]-L-tryptophan methylamide. *Cancer Res* 1994;54:4715–4718.
- Moss ML, Rasmussen FH. Fluorescent substrates for the proteinases ADAM17, ADAM10, ADAM8, and ADAM12 useful for high-throughput inhibitor screening. *Anal Biochem* 2007;366:144–148.
- Asakura M, Kitakaze M, Takashima S *et al*. Cardiac hypertrophy is inhibited by antagonism of ADAM12 processing of HB-EGF: metalloproteinase inhibitors as a new therapy. *Nat Med* 2002;8:35–40.
- Ichikawa Y, Miura T, Nakano A *et al*. The role of ADAM protease in the tyrosine kinase-mediated trigger mechanism of ischemic preconditioning. *Cardiovasc Res* 2004;62:167–175.
- Zhou BB, Peyton M, He B *et al*. Targeting ADAM-mediated ligand cleavage to inhibit HER3 and EGFR pathways in non-small cell lung cancer. *Cancer Cell* 2006;10:39–50.
- Hashimoto K, Higashiyama S, Asada H *et al*. Heparin-binding epidermal growth factor-like growth factor is an autocrine growth factor for human keratinocytes. *J Biol Chem* 1994;269:20060–20066.
- Chen CD, Podvin S, Gillespie E, Leeman SE, Abraham CR. Insulin stimulates the cleavage and release of the extracellular domain of Klotho by ADAM10 and ADAM17. *Proc Natl Acad Sci USA* 2007;104:19796–19801.
- Tanida S, Joh T, Itoh K *et al*. The mechanism of cleavage of EGFR ligands induced by inflammatory cytokines in gastric cancer cells. *Gastroenterology* 2004;127:559–569.
- Reizes O, Goldberger O, Smith AC *et al*. Insulin promotes shedding of syndecan ectodomains from 3T3-L1 adipocytes: a proposed mechanism for stabilization of extracellular lipoprotein lipase. *Biochemistry* 2006;45:5703–5711.
- Wang Y, Sul HS. Ectodomain shedding of preadipocyte factor 1 (Pref-1) by tumor necrosis factor  $\alpha$  converting enzyme (TACE) and inhibition of adipocyte differentiation. *Mol Cell Biol* 2006;26:5421–5435.
- Singh AB, Harris RC. Autocrine, paracrine and juxtacrine signaling by EGFR ligands. *Cell Signal* 2005;17:1183–1193.
- Serino M, Menghini R, Fiorentino L *et al*. Mice heterozygous for tumor necrosis factor- $\alpha$  converting enzyme are protected from obesity-induced insulin resistance and diabetes. *Diabetes* 2007;56:2541–2546.
- Gelling RW, Yan W, Al-Noori S *et al*. Deficiency of TNF $\alpha$  converting enzyme (TACE/ADAM17) causes a lean, hypermetabolic phenotype in mice. *Endocrinology* 2008;149:6053–6064.
- Uysal KT, Wiesbrock SM, Marino MW, Hotamisligil GS. Protection from obesity-induced insulin resistance in mice lacking TNF- $\alpha$  function. *Nature* 1997;389:610–614.
- Uysal KT, Wiesbrock SM, Hotamisligil GS. Functional analysis of tumor necrosis factor (TNF) receptors in TNF- $\alpha$ -mediated insulin resistance in genetic obesity. *Endocrinology* 1998;139:4832–4838.
- Schreyer SA, Chua SC Jr, LeBoeuf RC. Obesity and diabetes in TNF- $\alpha$  receptor-deficient mice. *J Clin Invest* 1998;102:402–411.
- Adachi H, Kurachi H, Homma H *et al*. Epidermal growth factor promotes adipogenesis of 3T3-L1 cell in vitro. *Endocrinology* 1994;135:1824–1830.
- Adachi H, Kurachi H, Homma H *et al*. Involvement of epidermal growth factor in inducing adiposity of age female mice. *J Endocrinol* 1995;146:381–393.
- Higashiyama S, Abraham JA, Klagsbrun M. Heparin-binding EGF-like growth factor stimulation of smooth muscle cell migration: dependence on interactions with cell surface heparan sulfate. *J Cell Biol* 1993;122:933–940.
- Miyegawa J, Higashiyama S, Kawata S *et al*. Localization of heparin-binding EGF-like growth factor in the smooth muscle cells and macrophages of human atherosclerotic plaques. *J Clin Invest* 1995;95:404–411.

## HDL/Apolipoprotein A-I Binds to Macrophage-Derived Progranulin and Suppresses its Conversion into Proinflammatory Granulins

Hanayuki Okura<sup>1,2,3</sup>, Shizuya Yamashita<sup>4</sup>, Tohru Ohama<sup>4</sup>, Ayami Saga<sup>1</sup>, Aya Yamamoto-Kakuta<sup>1</sup>, Yoko Hamada<sup>1</sup>, Nagako Sougawa<sup>1</sup>, Reiko Ohyama<sup>1</sup>, Yoshiki Sawa<sup>2</sup>, and Akifumi Matsuyama<sup>1</sup>

<sup>1</sup>Department of Somatic Stem Cell Therapy, Institute of Biomedical Research and Innovation, Foundation for Biomedical Research and Innovation, Kobe, Japan

<sup>2</sup>Division of Cardiovascular Surgery, Department of Surgery, Osaka University Graduate School of Medicine, Suita, Osaka, Japan

<sup>3</sup>Research Fellow of the Japan Society for the Promotion of Science, Tokyo, Japan

<sup>4</sup>Division of Cardiology, Department of Internal Medicine, Osaka University Graduate School of Medicine, Suita, Osaka, Japan

**Aim:** HDL has anti-inflammatory effects on macrophages, although the mechanism of action remains unclear. We hypothesized that HDL suppresses the conversion of macrophage-secreted factors into proinflammatory factors via binding, and tried to identify the factor that could form a complex with HDL and/or apolipoprotein (apo) A-I.

**Methods and Results:** In conditioned media obtained from human monocyte-derived macrophages, we found an apo A-I binding protein and identified the protein as progranulin/proepithelin/acrogranin/PCDGF. Co-immunoprecipitation analysis showing that progranulin binds and forms a complex with apo A-I and the presence of progranulin in the HDL fraction in the sera indicated that progranulin is a novel apolipoprotein. Conditioned media of HEK293 cells transfected with progranulin augmented the expression of TNF-alpha and IL-1-beta on macrophages, but these effects of progranulin were inhibited by co-incubation with HDL or apo A-I. Anti-progranulin antibodies also reduced the expression of TNF-alpha and IL-1-beta on macrophages. Granulins as conversion products derived from progranulin increased TNF-alpha and IL-1-beta expression and the effects were not suppressed by HDL.

**Conclusions:** Our results suggest that the anti-inflammatory effects of HDL on macrophages might be due to suppression of the conversion of progranulin into proinflammatory granulins by forming a complex.

*J Atheroscler Thromb, 2010; 17:000-000.*

**Key words;** HDL, Apolipoprotein A-I, Progranulin, Proepithelin, Acrogranin, PCDGF, Macrophage

### Introduction

Several pathological studies have shown that low high-density lipoprotein (HDL) levels are associated with plaque instability in patients with acute coronary syndrome<sup>1</sup>. Accordingly, the reverse cholesterol trans-

port system, in which excess cholesterol is extracted from atheromatous plaques, is considered important in stabilizing plaques and preventing plaque rupture<sup>2-3</sup>. A recent study reported that in addition to the reverse cholesterol system, HDL infusion could stabilize atheromatous plaque through its anti-inflammatory properties<sup>4</sup>.

The acute phase of a coronary event is associated with a significant fall in serum levels of apolipoprotein (apo) A-I (a major component of HDL) and HDL-C<sup>5</sup>. There is evidence that plasma HDL-C measured in the initial stage of the acute phase of coronary events predicts the risk of recurrent cardiovascular events over the ensuing 16 weeks<sup>6</sup>. We often expe-

Address for correspondence: Akifumi Matsuyama, Department of Somatic Stem Cell Therapy, Institute of Biomedical Research and Innovation, Foundation for Biomedical Research and Innovation, TRI305, 1-5-4, Minatojima-minamimachi, Chuo-ku, Kobe 650-0047, Japan

E-mail: akifumi-matsuyama@umin.ac.jp

Received: October 1, 2008

Accepted for publication: November 17, 2009

rience patients with acute coronary syndrome whose HDL levels are reduced before the occurrence of plaque instability<sup>4)</sup>.

Infiltration and accumulation of foam cells (macrophages) is a characteristic feature of atheromatous plaques<sup>7)</sup>. Once activated, macrophages secrete various pro-inflammatory cytokines and proteases, which could result in plaque instability and rupture<sup>7)</sup>. Are the anti-inflammatory effects of HDL mediated through suppression of the secretion of such cytokines from macrophages? The main theme of our research is to determine the mechanisms underlying the reduction of serum HDL during the acute phase of coronary events. In this study, we hypothesized that HDL modulates the expression levels of pro-inflammatory cytokines secreted by macrophages. Progranulin is here described as a macrophage-derived secretory factor, which is a pluripotent protein and a precursor of its proteolytic peptides, granulins, whose functional properties were different from their intact precursor in some cases<sup>8)</sup>, and whose pro-inflammatory properties were suppressed via binding to HDL.

## Materials and Methods

### Lipoprotein Isolation

Apo A-I was purchased from Sigma Aldrich (St. Louis, MO). HDL3 were isolated from human serum by ultracentrifugation at a density of 1.125–1.210 g/mL<sup>9)</sup>.

### Isolation of Human Monocyte-Derived Macrophages

Mononuclear cells were isolated from the buffy coats of plasma collected from healthy volunteers using density gradient centrifugation with Lymphoprep (Nycomed, Oslo, Norway). The cells were then cultured for 7 days, as described previously<sup>9)</sup>.

### Preparation of Conditioned Medium

A monolayer of macrophages was collected from 7-day culture and incubated in serum-free RPMI1640 for 24 h at 37°C. The conditioned medium was collected and replaced with fresh RPMI1640 every 24 hours for 5 days. The collected medium was centrifuged, and the supernatant was treated with benzamidine hydrochloride (Sigma) at a final concentration of 1 mM to protect against protease degradation.

### Ligand Blotting Analysis

The concentrated conditioned medium was separated under non-reducing conditions using 10–20% polyacrylamide gradient gels, transferred onto nitrocellulose membranes, and blotted with 5 µg/mL bioti-

nylated-apo A-I. After incubation with peroxidase-conjugated streptavidin, the blots were visualized with an ECL kit (Amersham Pharmacia Bioscience, Uppsala, Sweden).

### Purification of Apo A-I Binding Protein from Macrophage-Conditioned Medium

The conditioned medium (total volume, 20 L) was collected and then treated with 80% ammonium sulfate. The precipitate was dissolved in 2.5 mL, and then desalted and equilibrated into Tris-buffered saline (20 mmol/L Tris HCl, pH 7.4, and 135 mmol/L NaCl) using a PD-10 column (Amersham Pharmacia Biotech). The eluate was added to an apolipoprotein A-I-affinity column (Amino Link; Amersham Pharmacia Biotech), and allowed to stand overnight at 4°C. After vigorous washing with Tris buffer with 1 mol/L NaCl (20 mmol/L Tris/HCl, pH 7.4, and 1 mol/L NaCl), the binding proteins were eluted with 8 mol/L urea. The eluate was concentrated with Amicon Ultra-15 50,000 MWCO (Millipore, Bedford, MA) to ensure purity, and subjected to SDS-PAGE.

### Amino Acid Sequencing

The purified apo A-I-binding protein was applied for in-gel digestion with V8 endopeptidase, transferred to a polyvinylidene fluoride (PVDF) membrane, and stained with Coomassie brilliant blue (CBB) R-250. The three apparent fragmented bands were subjected to amino acid sequencing in a sequencer (Perkin Elmer-Cetus, Foster City, CA).

### Construction of Progranulin, Granulin A and Granulin B Expression Vector

The expression vectors of progranulin (aa 1-593, see RESULTS), myc-His-tagged progranulin and granulin were constructed from pcDNA3.1, as described previously<sup>10)</sup>. In short, cDNA obtained from human monocyte-derived macrophages underwent PCR using primer pairs 5'-aggaccgaggagtcggacgcaggcagacca-3' and 5'-tccgagtgggtcccagggtcgcagagtc-3', and for nested PCR, primer pairs 5'-gtcggactccggcagaccatgtggaccctg-3' and 5'-agggctcgcagagtcctcagactgtccctc-3'. The nested PCR product was digested with Bam HI and Xho I and the digested product was ligated into pcDNA3.1 pretreated with Bam HI and Xho I. The construct was used as a progranulin expression vector. To obtain myc-His tagged progranulin expression vector, cDNA obtained from human monocyte-derived macrophages underwent PCR using primer pairs 5'-aggaccgaggagtcggacgcaggcagacca-3' and 5'-tccgagtgggtcccagggtcgcagagtc-3', and for nested PCR, primer pairs 5'-gtcggactccggcagaccatgtggaccctg-3' and 5'-tccc-

tcacctctagagcagctgtctcaagg-3', and the nested PCR product was digested with Bam HI and Xba I and the digested product was ligated into pcDNA3.1/myc-His vector pretreated with Bam HI and Xba I. Human granulin A (aa 281-337) and B (aa 206-261) vectors were constructed with secretion being driven by the human progranulin signal peptide (aa 1-17).

### Immunoprecipitation

The vectors were transiently expressed in HEK293 cells using a Calcium Phosphate Transfection Kit (Invitrogen Corp., Carlsbad, CA, USA). Three days after transfection, HEK293 cells were incubated with conditioned medium containing apo A-I (final concentration 5  $\mu\text{g}/\text{mL}$ ) at 37°C for 30 min. The apo A-I-containing media were collected and immunoprecipitated with anti-progranulin antibody (clone N19; Santa Cruz Biotechnology, Santa Cruz, CA), pulled-down with protein G (Amersham Pharmacia Biotech), separated by reducing SDS-PAGE, and Western blotted with anti-apo A-I antibody, or the reverse. *In vitro* translated progranulin was produced using an *in vitro* translation system (Duo, Tokyo, Japan), and mixed with apo A-I at a final concentration of 5  $\mu\text{g}/\text{mL}$ . The mixture was then subjected to co-immunoprecipitation analysis.

### Immunoblotting Analysis

The conditioned medium was subjected to immunoblotting analysis with anti-progranulin monoclonal antibody (clone N-19; Santa Cruz Biotechnology). The blots were visualized after incubation with peroxidase-conjugated anti-mouse IgG antibody (DAKO, Denmark).

### Quantitative Real-Time PCR

The constructed expression vectors of progranulin, granulin A and granulin B, were transiently expressed in HEK293 cells using a Calcium Phosphate Transfection Kit (Invitrogen Corp.). Three days after transfection, the conditioned media were obtained and macrophages were incubated in conditioned media with or without HDL (10  $\mu\text{g}/\text{mL}$ ) or apo A-I (5  $\mu\text{g}/\text{mL}$ ) for 24 h. Total RNA was then isolated using RNeasy MINI kits (Qiagen, Hilden, Germany) according to the instructions provided by the manufacturer. For cDNA synthesis, 600 ng total RNA was reverse transcribed using SuperScript III RTase (Invitrogen, San Diego, CA). TaqMan probe and primers for progranulin, CD14, CD36, CD68, TNF-alpha, IL-1beta and GAPDH were purchased from Applied Biosystems (Assay ID: Hs00173570\_m1, Hs02621496\_S1, Hs01567186\_m1, Hs00154355\_m1, Hs99999043\_m1,

Hs99999029\_m1 and Hs00266705\_g1, respectively). Quantitative real-time PCR was performed using the ABI Prism 7900 Sequence Detector System (Applied Biosystems, Foster City, CA). The cDNA samples (10 ng in a total volume of 10  $\mu\text{L}$ ) were mixed with primers, probe and TaqMan Universal PCR Master Mix as described in the accompanying sheet supplied by the manufacturer (Applied Biosystems). PCR was conducted using the following settings: 50°C for 2 min, 95°C for 10 min and 40 cycles at 95°C for 15 s and 60°C for 1 min.

## Results

### Purification of Progranulin as Apo A-I Binding Protein

We first tested whether HDL suppresses the proinflammatory cytokines secreted by macrophages by forming complexes with them, and thus searched for hypothetical proteins. The conditioned media obtained from 7-day-cultured human macrophages were concentrated with the ammonium sulfate precipitation method, desalted and subjected to ligand blotting analysis using biotinylated-apo A-I as a ligand. After separating the media on SDS-PAGE under non-reducing conditions, we detected an apo A-I-binding protein with a MW of 130 kDa (**Fig. 1A**). To purify the protein, the concentrated medium was subjected to an affinity column with immobilized human apo A-I and we obtained a concentrated eluate. To ensure purity, 10  $\mu\text{g}$  proteins of the conditioned medium and 0.5  $\mu\text{g}$  of the eluted protein were subjected to SDS-PAGE. Silver staining showed a single band of 80 kDa protein (**Fig. 1B**).

In the next step, we obtained three polypeptide fragments after in-gel-digestion with V8 proteases. Next, the amino-terminal sequence of these polypeptides was determined. The amino acid sequences were "avacgdgh", "nattdllt" and "kapahls", respectively. All amino acid sequences were identical to those of progranulin (aa 89-96, 265-272 and 347-354, respectively).

To confirm that progranulin could bind to HDL, HDL fractions (0.5  $\mu\text{g}$ ) were applied for immunoblotting with anti-progranulin antibody (clone N19). As shown in **Fig. 1C**, progranulin was observed in the HDL fraction, and a small amount was observed in serum. As indicated in **Fig. 1A**, HDL binding protein had approximately 130kDa molecular weight in non-reducing conditions; however, MW of progranulin was approximately 80 kDa, as shown in **Fig. 1B**. To clarify these discrepancies, purified proteins by affinity column with immobilized human apo A-I were

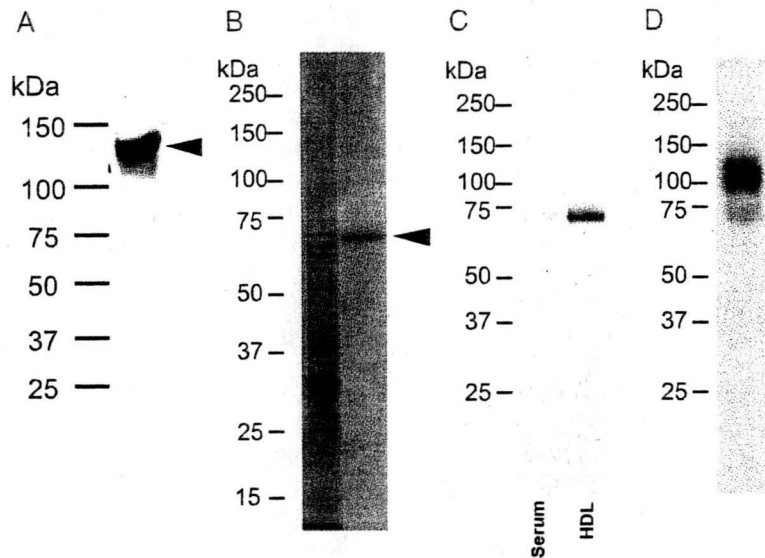


**Fig. 1.** Purification of apolipoprotein A-I binding protein from macrophage-conditioned medium.

(A) SDS-PAGE of purified apo A-I binding protein from macrophage-conditioned medium. The conditioned medium derived from human macrophages (150  $\mu$ g/lane) was subjected to 4/20% gradient SDS-PAGE under non-reducing conditions, and subjected to ligand blotting analyses with 5  $\mu$ g/mL biotinylated apo A-I.

(B) Ligand blotting of the purified apo A-I binding protein in macrophage-conditioned medium. The conditioned medium derived from macrophages was collected, concentrated, and then 10  $\mu$ g proteins of the conditioned medium were subjected to SDS-PAGE and silver staining (left lane). After purification of apo A-I binding protein, 0.5  $\mu$ g of the purified protein was used for SDS-PAGE and silver stained to ensure purity (right lane).

(C) Immunoblotting of HDL fraction with anti-progranulin. Human serum and HDL fractions (0.1  $\mu$ g) were applied for immunoblotting with anti-progranulin antibody (clone N19).

(D) Progranulin could form a homo-dimer. Proteins purified by affinity column with immobilized human apo A-I were applied for immunoblotting under non-reducing conditions. Progranulin-like immunoreactive bands were observed in 130 kDa and 80 kDa.

applied for immunoblotting in non-reducing conditions. Progranulin-like immunoreactive bands were observed in 130 kDa and 80 kDa (**Fig. 1D**), indicating that progranulin could form a homo-dimer.

#### Formation of Progranulin-Apo A-I Complex

To confirm the formation of progranulin-apo A-I complex, we performed co-immunoprecipitation analysis (**Fig. 2**). Progranulin-expressing conditioned medium treated with apo A-I was subjected immunoprecipitated with anti-apo A-I antibody to bring down apo A-I and then Western blotted with anti-progranulin antibody or the reverse (**Fig. 2A, B**). The two proteins were recovered simultaneously, indicating that progranulin binds apo A-I. To further confirm the formation of the protein complex, progranulin was trans-

lated *in vitro*, co-incubated with apo A-I and then subjected to co-immunoprecipitation analysis (**Fig. 2C, D**). Progranulin, *in vitro* translated under non-reducing conditions (**Fig. 2C, D**), was detected in apo A-I immunoprecipitates while apo A-I was identified in progranulin immunoprecipitates or the reverse. These results indicate that progranulin and apo A-I could bind each other.

#### Progranulin-Expressing Macrophages

Although we purified and identified progranulin as an apo A-I binding protein from conditioned media derived from macrophages, it is important to confirm that macrophages express and produce progranulin. As shown in **Fig. 3A**, macrophages expressed progranulin and the expression level was dependent on mac-



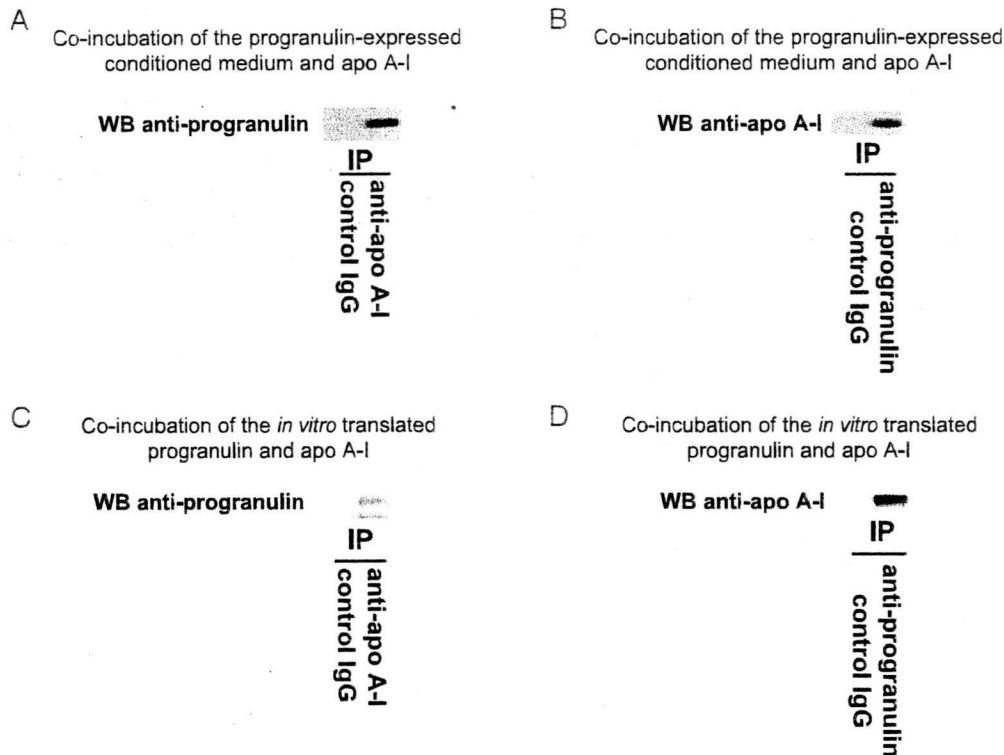


**Fig. 2.** Progranulin and apolipoprotein A-I form a complex.

(A) Formation of a protein complex from progranulin, transfected and secreted from HEK293 cells, and apolipoprotein A-I. The conditioned medium of HEK293 cells, transfected with pcDNA3.1 expression vector of progranulin, and apo A-I, was immunoprecipitated using rabbit anti-apo A-I antibody. Similar samples were immunoprecipitated using control rabbit IgG as a negative control. The precipitated samples were resolved by SDS-PAGE and blotted onto nitrocellulose membranes, which were incubated with anti-progranulin antibody, and then visualized.

(B) Formation of a protein complex from progranulin, transfected and secreted from HEK293 cells, and apolipoprotein A-I. The conditioned medium of HEK293 cells, transfected with pcDNA3.1 expression vector of progranulin, and apo A-I, was immunoprecipitated using rabbit anti-progranulin antibody. The precipitated samples were resolved by SDS-PAGE and blotted onto nitrocellulose membranes, which were incubated with anti-apo A-I antibody, and then visualized.

(C) Progranulin, translated under native but not reducing conditions, and apolipoprotein A-I form a complex. The *in vitro* translated progranulin and apo A-I were immunoprecipitated using rabbit anti-apo A-I antibody. Similar samples were immunoprecipitated using control rabbit IgG as a negative control. The precipitated samples were resolved by SDS-PAGE and blotted onto nitrocellulose membranes, which were incubated with anti-progranulin antibody (N19), and then visualized.

(D) Progranulin, translated under native but not reducing conditions, and apolipoprotein A-I form a complex. The *in vitro* translated progranulin and apo A-I were immunoprecipitated using rabbit anti-progranulin antibody. Similar samples were immunoprecipitated using control rabbit IgG as a negative control. The precipitated samples were resolved by SDS-PAGE and blotted onto nitrocellulose membranes, which were incubated with anti-apo A-I antibody, and then visualized.

rophage differentiation; gene expression was higher after 5-day culture. Next, we examined progranulin protein production by macrophages (**Fig. 3B**). After cultivation for the indicated time, macrophages were incubated without serum for 24 h and their conditioned media were blotted with anti-progranulin antibody. The production of progranulin protein by mac-

rophages increased in a macrophage differentiation-dependent manner, similar to the gene expression. To examine whether progranulin could augment the expression of progranulin itself, TNF-alpha and IL-1-beta, 7-day-cultured human macrophages were cultured for 24 hours with progranulin. As shown in **Fig. 3C**, progranulin increased the expression of pro-



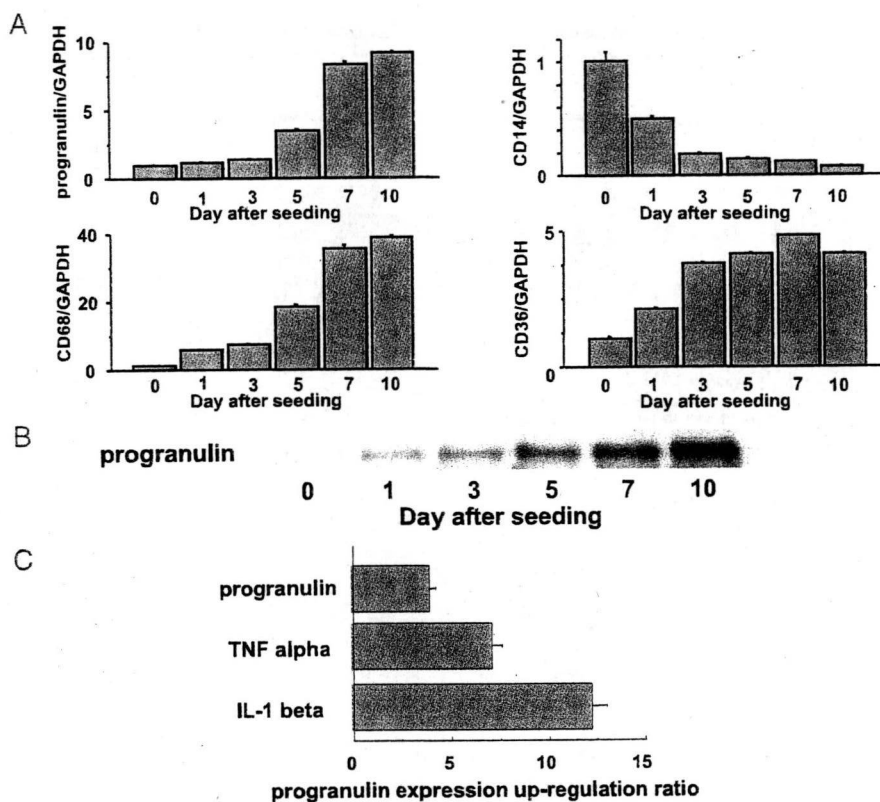


**Fig. 3.** Human monocyte-derived macrophages express and secrete progranulin into conditioned media.

(A) Expression of progranulin on macrophages is macrophage maturation-dependent. Human monocyte-derived macrophages expressed progranulin and the expression level was dependent on macrophage differentiation by quantitative PCR. Maturation of monocytes-macrophages was associated with over-expression of CD36 and CD68 and under-expression of CD14. Data are the mean  $\pm$  SE of 5 experiments.

(B) The amount of progranulin secreted by macrophages is macrophage maturation-dependent. Human monocyte-derived macrophages secreted progranulin into the conditioned media and the amount of progranulin protein increased with the differentiation of these cells.

(C) Autocrine regulation of progranulin production. Progranulin could augment the expression of progranulin itself, TNF- $\alpha$  (10 ng/mL) and IL-1- $\beta$  (10 ng/mL) on macrophages cultured with progranulin. Up-regulation of progranulin expression by progranulin itself, TNF- $\alpha$ , or IL-1- $\beta$  was observed. Data are the mean  $\pm$  SE of 5 experiments.

granulin itself, TNF- $\alpha$  and IL-1- $\beta$  (3.9-, 7.1- and 12.2-fold expressions, respectively).

#### Progranulin Activates Macrophages and HDL/Apo A-I Suppress as Such Activation

The production of cytokines by macrophages is often regulated in a paracrine or autocrine manner<sup>8)</sup>. Next, we examined whether progranulin had effects on macrophages and whether HDL and apo A-I suppress such effects of progranulin. TNF- $\beta$  and IL-1- $\alpha$  were selected in the present study as representative pro-inflammatory cytokines. Seven-day-cultured

macrophages were incubated with progranulin-expressing conditioned medium for 24 h, and TNF- $\alpha$  and IL-1- $\beta$  gene expression levels were examined by quantitative PCR using a TaqMan Probe (Fig. 4A). Progranulin augmented the expression levels of TNF- $\alpha$  and IL-1- $\beta$ , indicating that progranulin affects macrophages. To confirm the binding of progranulin and HDL/apo A-I, the supernatants of macrophages with progranulin-expressing conditioned medium, and apo A-I or HDL under the same conditions were applied for immunoprecipitation with anti-progranulin. The precipitated samples were resolved

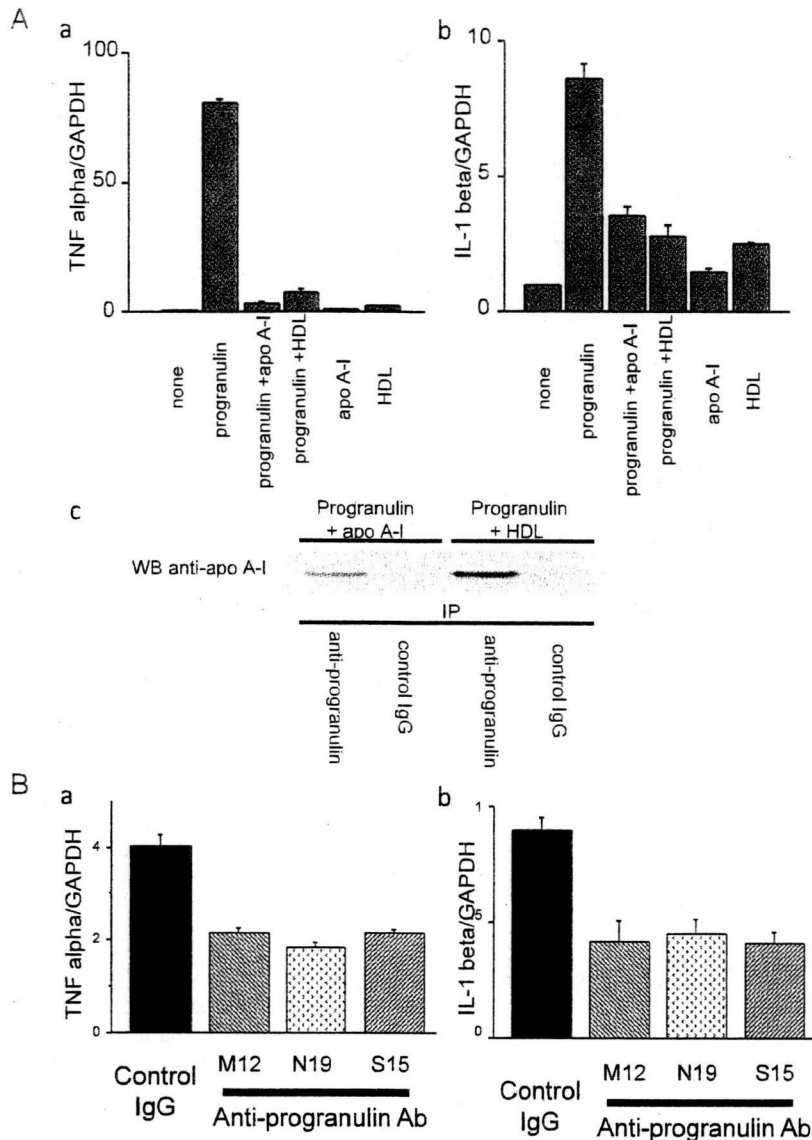


**Fig. 4.** Effects of progranulin on the expression levels of TNF-alpha and IL-1-beta in macrophages.

(A) Progranulin activated macrophages and HDL/apo A-I suppressed the effects. Seven-day-cultured macrophages were incubated with progranulin-expressing conditioned medium for 24 h and the expression levels of TNF-alpha (a) and IL-1beta (b) were examined with quantitative PCR using TaqMan Probe. Progranulin augmented the expressions of TNF-alpha and IL-1-beta. These properties of progranulin were suppressed by co-incubation with apo A-I (5  $\mu$ g/mL) or HDL (10  $\mu$ g/mL). Data are the mean  $\pm$  SE of 5 experiments. The supernatants of macrophages with progranulin-expressing conditioned medium, and apo A-I or HDL under the same conditions were applied for immunoprecipitation with anti-progranulin. The precipitated samples were resolved by SDS-PAGE and blotted onto nitrocellulose membranes, which were incubated with anti-apo A-I antibody, and then visualized (c).

(B) Anti-progranulin antibodies reduced the expression of TNF-alpha and IL-1beta. Macrophages were cultured in the conditioned medium with anti-progranulin antibody for 24 h. Compared to incubation with control IgG (100  $\mu$ g/mL), anti-progranulin antibody (clone M12, N9 and S15, 100  $\mu$ g/mL each) suppressed the expressions of TNF-alpha (a) and IL-1-beta (b). Data are the mean  $\pm$  SE of 5 experiments.

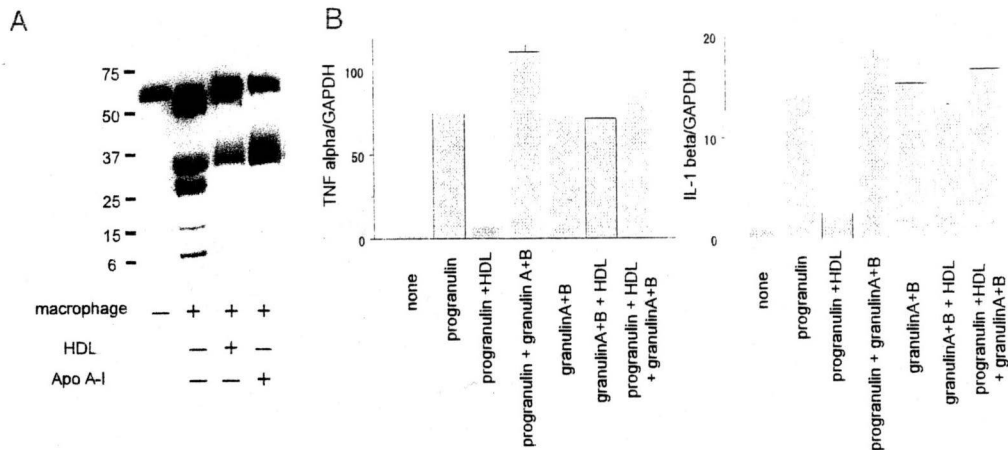


**Fig. 5.** Progranulin exerts its proinflammatory properties via conversion into granulins.

(A) Progranulin conversion by macrophages. C-terminal-myc-His-tagged progranulin was incubated with or without human macrophages for 24hr. Progranulin was degraded by macrophages and small degraded products were observed, but conversion was suppressed by incubation with HDL or apo A-I.

(B) Suppression of pro-inflammatory properties of progranulin by HDL via inhibition of conversion into granulins. Progranulin could increase the expression of pro-inflammatory cytokines, TNF-alpha and IL-1 beta, and this augmentation was suppressed by incubation with HDL (10  $\mu$ g/mL). On the other hand, the augmentation effect on the expression of TNF-alpha and IL-1 beta of granulin was not blocked by incubation with HDL. Data are the mean  $\pm$  SE of 4 experiments.

by SDS-PAGE and blotted onto nitrocellulose membranes, which were incubated with anti-apo A-I antibody, and then visualized (c). These results indicated that the effects of progranulin were suppressed by co-incubation with HDL or apo A-I via binding.

#### Anti-Progranulin Antibodies Reduce the Expression of TNF-Alpha and IL-1Beta

To examine whether the effect of progranulin on macrophages is autocrine in nature, fully differentiated macrophages were cultured with anti-progranulin antibody for 24 h. Compared to incubation with control IgG, anti-progranulin antibody (clone M12, N9 and S15) suppressed the expression of TNF-alpha and IL-1-beta (Fig. 4B). These results suggest that progranulin is secreted by macrophages and its effect is autocrine in nature, indicating that progranulin is an autoactivating molecule.

#### Progranulin Exerts its Properties Via Conversion into Proinflammatory Granulins

We examine whether progranulin could be converted into fragments by macrophages and exerted its properties via conversion into proinflammatory granulins. C-terminal-myc-His-tagged progranulin construct was transfected into HEK293T, and the conditioned media were incubated with or without human macrophages for 24 hr. Probond beads were added to

the media to capture His-tagged proteins. Next, the incubated probond beads were applied for immunoblotting with anti-myc antibody. C-terminal-myc-His-tagged progranulin was degraded by macrophages and small degraded products were observed but not with HDL incubation (Fig. 5A), indicating that progranulin could be converted by macrophages.

Next, we examined whether granulin could increase the expressions of TNF-alpha and IL-1-beta, and the increment could be suppressed by HDL (Fig. 5B). Progranulin could increase the expressions of pro-inflammatory cytokines, TNF-alpha and IL-1-beta, and this augmentation was suppressed by incubation with HDL. On the other hand, the augmentation effect on the expressions of TNF-alpha and IL-1-beta of granulin was not blocked by incubation with HDL (Fig. 5B, left and right panels, respectively). These results suggested that progranulin could exert its pro-inflammatory properties via conversion into granulins, and that HDL could suppress the pro-inflammatory properties of progranulin by inhibiting the conversion into granulins.

#### Discussion

Progranulin, a PC-cell-derived growth factor (PCDGF), or acrogranin, was purified from the conditioned media of transformed cell lines as an auto-

crine growth factor<sup>11</sup>. It is reported to be involved in cancer progression<sup>8</sup>, development<sup>12</sup>, wound healing<sup>13</sup>, and myeloid cell proliferation<sup>14</sup>, whereas mutation of progranulin causes frontotemporal dementia<sup>15, 16</sup>. In the present study, we demonstrated that the macrophage-secreted factor was approximately 130 kDa, while the purified protein identified as progranulin was 80 kDa. The 130-kDa HDL binding protein might be a homodimer or heteromer that includes progranulin, which is known to be glycosylated and to have disulfide bonds<sup>11</sup>.

Ong and colleagues<sup>14</sup> used myeloid cell lines and reported the overexpression of progranulin in macrophages and monocyte-derived dendritic cells, and that the level of expression was dependent on cell differentiation. Our results also demonstrated that the differentiation of human monocyte-derived macrophages was associated with increased expression levels of progranulin and that progranulin expression was regulated in an autocrine fashion in human monocyte-derived macrophages. We also demonstrated that apo A-I, the major component of HDL, suppressed the conversion of progranulin into pro-inflammatory granulins on human peripheral monocyte-derived macrophages. This is in agreement with others, who indicated that the protein precursor (progranilin) and its processed fragments (granulins) are both bioactive and pro-inflammatory<sup>8</sup>.

The role of progranulin in the inflammatory process was initially explored in research on the functions of secretory leukocyte protease inhibitor (SLPI) in wounds<sup>10</sup>. Using a yeast two-hybrid approach, with SLPI as the bait, Zhu and colleagues<sup>10</sup> demonstrated that progranulin is associated with SLPI<sup>10</sup>. This interaction was confirmed by immunoprecipitation experiments demonstrating that progranulin regulates inflammation through a tripartite loop with SLPI, which protects progranulin from proteolysis, and elastase, which digests progranulin between granulin/epithelin domains, generating smaller granulin/epithelin peptides. SLPI blocks this proteolysis, by inhibiting both elastase activity directly and by binding progranulin and sequestering it from the enzyme<sup>10</sup>. Intact progranulin is anti-inflammatory through the inhibition of certain actions of TNF-alpha, while proteolytic peptides may stimulate the production of pro-inflammatory cytokines, such as IL-8<sup>8</sup>. We suppose that HDL/apo A-I have anti-inflammatory effects on macrophages through the formation of a complex with progranulin and prevent the conversion of progranulin into granulins by elastase secreted by macrophages such as SLPI, which is reported as a neutrophil-derived anti-inflammatory factor<sup>10</sup>. In this study,

the possibility could be not rejected that progranulin binds HDL particles itself but free apoA-I is dissociated from HDL, which is just a reserve of apoA-I *in vivo* according to the limitations of the experimental conditions. In the near future, our colleagues will demonstrate which of apo A-I, lipid-free apo A-I dissociated from HDL, apo A-I in pre-beta HDL or apo A-I in HDL will bind to progranulin *in vivo*.

An unstable and subsequently ruptured atherosclerotic coronary plaque superimposed on thrombosis constitutes the most common pathological background of acute coronary syndrome<sup>7</sup>. High levels pro-inflammatory cytokines have been found in unstable angina, possibly supporting their role in acute coronary syndrome<sup>7</sup>. Cytokines induce their own expression in an autocrine fashion and also the expression of various adhesion molecules via the cellular transcription factor NF-kappaB<sup>17</sup>. Monocytes adhering to the endothelium and penetrating the plaque (macrophages) are activated by several paracrine/autocrine pro-inflammatory mediators. At this crucial stage, activated macrophages then synthesize and secrete pro-inflammatory cytokines TNF-alpha and IL-1-beta<sup>7</sup>. The human and murine progranulin promoter contains potential inflammation-related promoter elements<sup>18, 19</sup>. Furthermore, TNF-alpha and IL-1-beta activate progranulin gene expression through the NF-kappaB system<sup>18, 19</sup>. The progranulin-granulin loop might play a role in autoactivation of macrophages. Given its actions in atherosclerosis, progranulin may prove a useful clinical target, both for prognosis and therapy.

In summary, we identified progranulin/proepithelin/acrogranin/PCDGF as a macrophage-derived factor whose properties were suppressed by binding to HDL/apo A-I. The normal function of progranulin is complex; the full-length form of the protein has both trophic and anti-inflammatory activities, whereas proteolytic cleavage generates granulin peptide that promotes inflammatory activity. Based on our results, we propose that HDL prevents the conversion of progranulin into its degraded proinflammatory products, granulins; however, the mechanisms involved in HDL-induced suppression of the pro-inflammatory effects of progranulin have not fully elucidated. Further studies are necessary to identify these mechanisms.

### Acknowledgment

This work was supported in part by grants from Kobe Translational Research Cluster, the Knowledge Cluster Initiative, Ministry of Education, Culture,

Sports, Science and Technology and by the Japan Heart Foundation/Pfizer Grant for Research on Hypertension, Hyperlipidemia and Vascular Metabolism for Akifumi Matsuyama.

#### References

- 1) Brewer HB Jr: HDL metabolism and the role of HDL in the treatment of high-risk patients with cardiovascular disease. *Curr Cardiol Rep*, 2007; 9: 486-492
- 2) Yamashita S, Hirano K, Sakai N, Matsuzawa Y: Molecular biology and pathophysiological aspects of plasma cholesteryl ester transfer protein. *Biochim Biophys Acta*, 2000; 1529: 257-275
- 3) Yokoyama S: ABCA1 and biogenesis of HDL. *J Atheroscler Thromb*, 2006; 13: 1-15
- 4) Ansell BJ, Watson KE, Fogelman AM, Navab M, Fonarow GC: High-density lipoprotein function. *Recent advances. J Am Coll Cardiol*, 2005; 46: 1792-1798
- 5) Fresco C, Maggioni AP, and LATIN Investigators: Variations in lipoprotein levels after myocardial infarction and unstable angina: the LATIN trial. *Ital Heart J*, 2002; 3: 587-592
- 6) Olsson AG, Schwartz GG, Szarek M, Sasiela WJ, Ezekowitz MD, Ganz P, Oliver MF, Waters D, Zeiher A: High-density lipoprotein, but not low-density lipoprotein cholesterol levels influence short-term prognosis after acute coronary syndrome: results from the MIRACL trial. *Eur Heart J*, 2005; 26: 890-896
- 7) Chapman MJ: From pathophysiology to targeted therapy for atherothrombosis: a role for the combination of statin and aspirin in secondary prevention. *Pharmacol Ther*, 2007; 113: 184-196
- 8) He Z, Bateman A: Progranulin (granulin-epithelin precursor, PC-cell-derived growth factor, acrogranin) mediates tissue repair and tumorigenesis. *J Mol Med*, 2003; 81: 600-612
- 9) Matsuyama A, Yamashita S, Sakai N, Maruyama T, Okuda E, Hirano K, Kihara S, Hiraoka H, Matsuzawa Y: Identification of a GPI-anchored type HDL-binding protein on human macrophages. *Biochem Biophys Res Commun*, 2000; 272: 864-871
- 10) Zhu J, Nathan C, Jin W, Sim D, Ashcroft GS, Wahl SM, Lacomis L, Erdjument-Bromage H, Tempst P, Wright CD, Ding A: Conversion of proepithelin to epithelins: roles of SLP1 and elastase in host defense and wound repair. *Cell*, 2002; 111: 867-878
- 11) Ong CH, Bateman A: Progranulin (granulin-epithelin precursor, PC-cell derived growth factor, acrogranin) in proliferation and tumorigenesis. *Histol Histopathol*, 2003; 18: 1275-1288
- 12) Díaz-Cueto L, Stein P, Jacobs A, Schultz RM, Gerton GL: Modulation of mouse preimplantation embryo development by acrogranin (epithelin/granulin precursor). *Dev Biol*, 2000; 217: 406-418
- 13) He Z, Ong CH, Halper J, Bateman A: Progranulin is a mediator of the wound response. *Nat Med*, 2003; 9: 225-229
- 14) Ong CH, He Z, Kriazhev L, Shan X, Palfree RG, Bateman A: Regulation of progranulin expression in myeloid cells. *Am J Physiol Regul Integr Comp Physiol*, 2006; 291: R1602-1612
- 15) Baker M, Mackenzie IR, Pickering-Brown SM, Gass J, Rademakers R, Lindholm C, et al: Mutations in progranulin cause tau-negative frontotemporal dementia linked to chromosome 17. *Nature*, 2006; 442: 916-919
- 16) Cruts M, Gijselinck I, van der Zee J, Engelborghs S, Wils H, Pirici D, et al: Null mutations in progranulin cause ubiquitin-positive frontotemporal dementia linked to chromosome 17q21. *Nature*, 2006; 442: 920-924
- 17) Shin WS, Szuba A, Rockson SG: The role of chemokines in human cardiovascular pathology: enhanced biological insights. *Atherosclerosis*, 2002; 160: 91-102
- 18) Bhandari V, Daniel R, Lim PS, Bateman A: Structural and functional analysis of a promoter of the human granulin/epithelin gene. *Biochem J*, 1996; 319: 441-447
- 19) Baba T, Nemoto H, Watanabe K, Arai Y, Gerton GL: Exon/intron organization of the gene encoding the mouse epithelin/granulin precursor (acrogranin). *FEBS Lett*, 1993; 322: 89-94

## Original Article

## Significance of Measuring Serum Concentrations of Remnant Lipoproteins and Apolipoprotein B-48 in Fasting Period

Itsuko Sato<sup>1</sup>, Yuichi Ishikawa<sup>2</sup>, Ai Ishimoto<sup>2</sup>, Shiho Katsura<sup>2</sup>, Atsushi Toyokawa<sup>2</sup>, Fujio Hayashi<sup>1</sup>, Seiji Kawano<sup>1</sup>, Yoshio Fujioka<sup>3</sup>, Shizuya Yamashita<sup>4</sup>, and Shunichi Kumagai<sup>1,5</sup>

<sup>1</sup>Department of Clinical Laboratory, Kobe University Hospital, Kobe, Japan

<sup>2</sup>Faculty of Health Sciences, Kobe University Graduate School of Health Sciences, Kobe, Japan

<sup>3</sup>Faculty of Nutrition, Kobegakuin University, Kobe, Japan

<sup>4</sup>Department of Cardiovascular Medicine, Osaka University Graduate School of Medicine, Osaka, Japan

<sup>5</sup>Department of Clinical Pathology and Immunology, Kobe University Graduate School of Medicine, Kobe, Japan

**Aim:** To characterize lipid profiles conveniently in the fasting period to detect postprandial hyperlipidemic subjects, we measured the concentrations of lipids, including remnant lipoproteins and apoB-48, before and after loading the test meal in 24 normolipidemic subjects.

**Methods:** We examined remnant-like particle-cholesterol and -triglyceride (RLP-C, RLP-TG) by the immune adsorption method, RemL-C by the newly developed homogeneous method, and apoB-48 by chemiluminescence enzyme immunoassay.

**Results:** After loading, TG, RemL-C, RLP-C, RLP-TG, and apoB-48 concentrations were elevated. Twenty subjects had only a slight elevation of TG (low TG group) after loading, while 4 subjects showed apparent increase of TG (more than 150 mg/dL, high TG group). In the fasting period, the high TG group had significantly higher serum concentrations of TG and RemL-C than the low TG group. Although not significant, RLP-C, RLP-TG and apoB-48 concentrations in the high TG group were also higher than in the low TG group. After loading, serum concentrations of TG, RemL-C, RLP-C, RLP-TG, and apoB-48 increased significantly more in the high TG group than in the low TG group.

**Conclusion:** In conclusion, TG, RemL-C, RLP-C, RLP-TG, and apoB-48 concentrations in the fasting period may be suitable for detecting postprandial hyperlipidemic subjects.

*J Atheroscler Thromb, 2009; 16:12-20.*

**Key words:** Postprandial hyperlipidemia, RLP-C, RemL-C, Small, dense LDL-C

### Introduction

Since Zilversmit's proposal of the significance of postprandial hyperlipidemia, many studies have investigated the role of remnant lipoproteins in the pathogenesis of atherosclerosis, and have identified a delay in their removal from blood as an independent risk factor<sup>1-6</sup>. In fact, high concentrations of remnant-like

particle (RLP)-cholesterol (RLP-C) predict coronary events in patients with CAD, independent of traditional coronary risk factors<sup>7-9</sup>.

In normal humans, the postprandial hyperlipidemic period is about 4-6 hours, but in individuals with certain dyslipidemia, this period may be increased beyond 6 hours<sup>3,4</sup>. Of note, impaired removal of chylomicron remnants in the liver potentially induces longer retention times for these lipoproteins in blood circulation. Moreover, it is important to recognize that dietary lipid is transferred to various parts of the body via plasma lipoproteins after food ingestion.

In the postprandial period, we can observe the elevation of triglyceride (TG)-rich lipoproteins, which include chylomicrons, very-low-density lipoproteins

Address for correspondence: Yoshio Fujioka, Laboratory of Nutritional Physiology, Faculty of Nutrition, Kobegakuin University 518 Arise, Ikawadani-cho, Nishi-ku, Kobe, 651-2180, Japan

E-mail: fujioka@nutr.kobegakuin.ac.jp

Received: May 30, 2008

Accepted for publication: September 22, 2008

(VLDL), and their remnants, in the blood circulation. Nascent chylomicrons, synthesized by enterocytes, have a high TG-to-cholesterol mass ratio, and consist primarily of apolipoprotein (apo) B-48 and apoA-I<sup>10, 11</sup>. After acquiring apoC-II and apoE, chylomicrons bind to lipoprotein lipase (LPL), which induces lipolysis of TG in chylomicrons. TG depletion results in a size reduction, and is referred to as chylomicron remnants, or "remnants". Finally, chylomicron remnants are cholesteryl ester-rich and retain apoB-48 and apoE<sup>12, 13</sup>. VLDL produced by hepatocytes are also hydrolyzed by LPL like chylomicrons, and become VLDL remnants containing apoB-100 and apoE.

Although it has been difficult clinically to distinguish exogenous lipids (chylomicrons and their remnants) from endogenous lipids (VLDL and their remnants), it recently became possible to conveniently measure the serum B-48 concentration<sup>14</sup>. In the present study, to characterize the lipid profiles conveniently in the fasting period to detect postprandial hyperlipidemic subjects, we measured the concentrations of lipids, including remnant lipoproteins and apoB-48, before and after loading the test meal in normolipidemic subjects.

## Subjects and Methods

### Subjects and Physical Examination

We recruited healthy subjects [ $n=24$ ; male/female, 11/13; mean  $\pm$  standard deviation (SD), 21.5  $\pm$  1.2 years old] who had never been treated or taken any drugs at least 3 months before the study. All subjects gave their informed consent to participate in the study. The study protocol was carried out according to the Declaration of Helsinki.

Blood pressure was measured twice by the same observer using a standard mercury sphygmomanometer after the subject had rested in a supine position for 30 min. Waist circumference of subjects was measured<sup>15</sup>. Body mass index (BMI) was calculated by dividing body weight by the square of the height ( $\text{kg}/\text{m}^2$ ).

### Study Protocol

We used a test meal containing carbohydrate, fat, and protein, which was developed for the assessment of both postprandial hyperglycemia and hyperlipidemia by the Japanese Diabetes Society (Test meal A). This test meal consists of cream of chicken soup, biscuit, and custard pudding. The total calories is 450 kcal, including carbohydrate 57.6 g (51.4% in energy balance), protein 17.2 g (15.3%), fat 16.6 g (33.3%), which is a slightly higher percentage of fat than in the usual Japanese breakfast (20–25%). Blood samples

were obtained at 9–10 AM after a 12-hour fast and 1, 2, 4, 6, and 8 hours after ingestion of the test meal.

### Blood Sampling and Analysis

Serum concentrations of TG, total cholesterol, high-density lipoprotein (HDL)-cholesterol (HDL-C) and low-density lipoprotein (LDL)-cholesterol (LDL-C) were determined by enzymatic methods (Kyowa Medex, Tokyo, Japan): plasma oxidized LDL concentration by enzyme-linked immunosorbent assay (Kyowa Medex); serum concentrations of apoA-I, apoA-II, apoB, apoC-II, apoC-III, and apoE by turbidimetric immunoassay methods (Nittobo, Tokyo, Japan); serum apoB-48 concentration by chemiluminescence enzyme immunoassay (Fujirebio, Tokyo, Japan)<sup>14</sup>; serum small, dense-LDL-cholesterol (sd-LDL-C) concentration by the precipitation method (Denka Seiken, Tokyo, Japan)<sup>16</sup>; serum concentrations of RLP-C and RLP-TG by the immune adsorption method (JIMRO II, Otsuka Pharmaceutical, Tokyo, Japan)<sup>17</sup>; serum remnant lipoprotein cholesterol (RemL-C) concentration by homogenous assay (MetaboLead RemL-C, Kyowa Medex)<sup>18</sup>; serum high sensitivity C-reactive protein (hs-CRP) concentration by nephelometry method (Dade Behring, Deerfield, IL); plasma glucose concentration and glycosylated hemoglobin A<sub>1c</sub> (HbA<sub>1c</sub>) by HPLC; and serum insulin concentrations by enzyme immunoassay, respectively.

### Agarose Gel Electrophoresis Analysis

Samples were subjected to lipoprotein analysis using agarose gel electrophoresis (Rapid Electrophoresis; Helena Laboratories, Beaumont, Texas), with 15 min of electrophoresis at 400 volts and 20°C. After staining with cholesterol and TG reagent, elution profiles were analyzed by an automatic densitometer, Chol/Trig Combo™ (Helena Kenkyusho, Saitama, Japan)<sup>19</sup>. Contents of cholesterol and TG in each fraction were calculated with total lipids and the area under the curve according to the report by Kido *et al.*<sup>20</sup>. Moreover, the ratios of cholesterol to TG in HDL and LDL fractions were calculated and compared with those in healthy volunteers reported previously (mean  $\pm$  SD; HDL, 5.8  $\pm$  2.0; LDL, 4.9  $\pm$  1.3)<sup>21</sup>.

### Statistical Analysis

Values are expressed as the mean  $\pm$  SD. Statistical significance of data was evaluated using either the Mann-Whitney *U*-test or Welch's *t*-test. Correlations between apoB-48 and other parameters were calculated using the formula for Pearson's correlation coefficient. Responses to the test meal were compared by analysis of variance (ANOVA) for repeated measures.



Table 1. Glucose and lipid parameters before and after loading the test meal

	0	1h	2h	4h	6h	8h
Plasma glucose (mg/dL)	89.4 ± 4.7	104.5 ± 19.2**	89.2 ± 11.5	85.3 ± 4.8**	85.2 ± 4.5**	85.1 ± 5.0**
Insulin (μU/mL)	6.1 ± 2.9	53.7 ± 27.5**	24.6 ± 16.4**	5.1 ± 2.2	4.1 ± 1.3*	3.7 ± 1.4*
TG (mg/dL)	65.6 ± 25.5	86.9 ± 38.2*	95.7 ± 47.4*	77.1 ± 32.6	60.7 ± 19.2	52.2 ± 16.8*
TC (mg/dL)	182.6 ± 32.2	181.5 ± 33.8	179.8 ± 32.4	181.4 ± 30.8	184.2 ± 31.7	189.5 ± 33.3
LDL-C (mg/dL)	100.0 ± 25.6	97.8 ± 25.7	96.8 ± 25.4	97.9 ± 24.4	101.1 ± 25.2	104.3 ± 26.2
HDL-C (mg/dL)	70.0 ± 14.3	67.8 ± 14.2	67.2 ± 13.1	68.0 ± 14.1	70.1 ± 14.9	72.5 ± 15.2
RemL-C (mg/dL)	3.5 ± 1.6	3.9 ± 1.9	4.0 ± 2.1	3.7 ± 2.1	3.1 ± 1.3	2.9 ± 1.1
RPL-C (mg/dL)	3.1 ± 1.2	4.4 ± 2.0*	4.7 ± 2.6*	3.8 ± 1.7	3.0 ± 1.3	2.8 ± 0.9
RLP-TG (mg/dL)	15.8 ± 2.6	24.8 ± 14.6*	30.4 ± 23.6*	20.1 ± 8.7	15.2 ± 0.7*	15.1 ± 0.2*
Sd-LDL-C (mg/dL)	21.4 ± 8.9	17.3 ± 5.8	17.1 ± 6.9	17.0 ± 5.7	17.5 ± 5.9	17.8 ± 5.8
Oxidized LDL (U/mL)	6.7 ± 4.9	6.1 ± 4.4	6.6 ± 5.5	6.5 ± 4.8	6.8 ± 4.7	7.1 ± 4.9
ApoA-I (mg/dL)	164.0 ± 27.0	161.8 ± 28.0	161.3 ± 25.0	162.5 ± 26.7	165.5 ± 26.7	168.2 ± 28.1
ApoA-II (mg/dL)	38.9 ± 7.1	38.5 ± 7.4	38.0 ± 6.9	38.5 ± 7.0	38.7 ± 7.1	39.3 ± 7.1
ApoB (mg/dL)	67.5 ± 14.2	66.3 ± 14.8	66.2 ± 14.0	66.8 ± 13.6	68.5 ± 13.9	70.5 ± 14.2
ApoB-48 (μg/mL)	3.2 ± 2.1	6.2 ± 3.1**	6.1 ± 3.4**	5.2 ± 2.9**	3.6 ± 2.1	3.0 ± 1.7
ApoC-II (mg/dL)	3.1 ± 1.1	3.2 ± 1.2	3.2 ± 1.2	3.2 ± 1.1	3.2 ± 1.1	3.2 ± 1.1
ApoC-III (mg/dL)	9.4 ± 2.5	9.9 ± 2.6	9.5 ± 2.6	9.3 ± 2.4	9.1 ± 2.3	9.3 ± 2.4
ApoE (mg/dL)	4.6 ± 1.0	4.5 ± 1.0	4.4 ± 1.0	4.4 ± 1.0	4.3 ± 0.9	4.4 ± 0.9

Values are expressed as the mean ± SD, \* $p < 0.05$ , \*\* $p < 0.01$  (vs. 0 time) by Mann-Whitney *U*-test. TG: triglyceride, TC: total cholesterol, LDL-C: low-density lipoprotein-cholesterol, HDL-C: high density lipoprotein-cholesterol, RemL-C: remnant lipoprotein cholesterol measured with "Metabo-Lead RemL-C", RLP-C: remnant-like particle-cholesterol measured with "JIMRO II", RLP-TG: remnant-like particle-triglyceride, Sd-LDL-C: small, dense-LDL-cholesterol, Apo: apolipoprotein.

Data under the threshold of RLP-C (<2.0 mg/dL) or RLP-TG (<15 mg/dL) were treated as 2.0 mg/dL or 15 mg/dL, respectively. Statistical analysis was performed using Stat Flex ver.5.0 software (Artec, Osaka, Japan). Two-tailed values of  $p < 0.05$  were considered significant.

## Results

### Characteristics of Subjects

Subject characteristics are as follows (mean ± SD): BMI, 20.7 ± 1.7 kg/m<sup>2</sup>; waist circumferences, 72.3 ± 4.2 cm in men and 65.7 ± 4.5 cm in women; HbA<sub>1c</sub>, 4.9 ± 0.2%; hsCRP, 0.04 ± 0.02 mg/dL.

### Fasting and Postprandial Concentrations of Lipids in Total Subjects

Table 1 shows the changes of lipid concentrations before and after loading the test meal in all subjects. In the fasting period (time 0), concentrations of all parameters were within normal limits or low ranges; however, there were significant correlations between apoB-48 concentration and TG, RemL-C, RLP-C, RLP-TG, apoC-II, or apoC-III concentration (Table 2), indicating that intestine-derived lipoproteins were present in the circulation and had charac-

teristics of remnants even in the fasting period in normolipidemic subjects.

After loading the test meal, TG, RLP-C, RLP-TG, and apoB-48 concentrations elevated significantly compared with before loading (Table 1). TG, RLP-C, and RLP-TG concentrations peaked at 2 hours, and were restored to the baseline within 4 hours. ApoB-48 concentrations peaked at 1 hour, and returned to basal levels at 6 hours. RemL-C concentrations also peaked at 2 hours and were restored within 6 hours, but this elevation had no significance. On the other hand, the concentrations of TC, HDL-C, LDL-C, sd-LDL-C, oxidized LDL, apoA-I, apoA-II, apoB, apoC-II, apoC-III, and apoE were not elevated. Sd-LDL-C concentrations decreased below the basal levels during the study without statistical significance.

### Comparison of Fasting Lipid Concentrations between High and Low TG Groups

In the results of the loading test, we noticed that some subjects showed apparent increases of TG at 2 hours as peak values, and others showed only a slight elevation. We therefore established two groups by TG values at 2 hours, and designated subjects with <150 mg/dL of TG ( $n=20$ ) as the low TG group and subjects with >150 mg/dL of TG ( $n=4$ ) as the high TG

Table 2. Correlation between apoB-48 concentration and other parameters in fasting period

	<i>r</i>	<i>P</i>
Plasma glucose (mg/dL)	0.236	0.2661
Insulin ( $\mu$ U/mL)	0.042	0.8448
TG (mg/dL)	0.791	<0.0001
TC (mg/dL)	0.287	0.1743
LDL-C (mg/dL)	0.301	0.1526
HDL-C (mg/dL)	-0.081	0.7065
RemL-C (mg/dL)	0.811	<0.0001
RLP-C (mg/dL)	0.768	<0.0001
RLP-TG (mg/dL)	0.745	<0.0001
Sd-LDL-C (mg/dL)	0.367	0.0776
Oxidized LDL (mg/dL)	-0.150	0.4832
ApoA-I (mg/dL)	0.016	0.9395
ApoA-II (mg/dL)	0.290	0.1693
ApoB (mg/dL)	0.282	0.1820
ApoC-II (mg/dL)	0.689	0.0002
ApoC-III (mg/dL)	0.534	0.0071
ApoE (mg/dL)	0.189	0.3764
hs-CRP (mg/L)	0.253	0.2321

Correlations between apoB-48 and other parameters were calculated using the formula for Pearson's correlation coefficient. TG: triglyceride, TC: total cholesterol, LDL-C: low-density lipoprotein-cholesterol, HDL-C: high density lipoprotein-cholesterol, RemL-C: remnant lipoprotein cholesterol measured with "MetaboLead RemL-C", RLP-C: remnant-like particle-cholesterol measured with "JIMRO II", RLP-TG: remnant-like particle-triglyceride, Sd-LDL-C: small, dense-LDL-cholesterol, Apo: apolipoprotein, hs-CRP: high sensitivity-C-reactive protein.

group. The peak concentrations of TG in the low TG group were  $78.4 \pm 27.6$  mg/dL, whereas those in the high TG group were  $182.5 \pm 33.7$  mg/dL.

First, we compared the profiles and lipid parameters in the fasting period between the two groups (Table 3). The high TG group had significantly higher serum concentrations of TG and RemL-C than the low TG group. Although not significant, RLP-C, RLP-TG and apoB-48 concentrations in the high TG group were also higher than in the low TG group. There were no significant differences in the profiles, including age, BMI, and abdominal circumference between the two groups.

### Comparison of Postprandial Concentrations between High and Low TG Groups

Fig. 1 demonstrates the sequential changes of parameters in lipids before and after loading the test meal in each group. Serum concentrations of TG, RemL-C, RLP-C, RLP-TG, and apoB-48 significantly increased more in the high TG group than in the low TG group,

Table 3. Comparison of clinical characteristics and fasting concentrations of glucose and lipid parameters between two groups

	High TG group ( <i>n</i> =4)	Low TG group ( <i>n</i> =20)	<i>P</i>
Age (years old)	22.0 $\pm$ 2.5	21.4 $\pm$ 0.9	0.6695
BMI (kg/m <sup>2</sup> )	22.0 $\pm$ 2.2	20.4 $\pm$ 1.5	0.2975
Abdominal circumference (cm)	73.5 $\pm$ 5.7	67.8 $\pm$ 5.2	0.1334
Hs-CRP (mg/dL)	0.06 $\pm$ 0.02	0.04 $\pm$ 0.02	0.1655
HbA <sub>1c</sub> (%)	5.0 $\pm$ 0.2	4.8 $\pm$ 0.2	0.3018
Plasma glucose (mg/dL)	83.0 $\pm$ 4.8	91.0 $\pm$ 3.6	0.0719
Insulin ( $\mu$ U/mL)	6.3 $\pm$ 2.6	6.1 $\pm$ 3.0	0.9060
TG (mg/dL)	109.5 $\pm$ 15.8	56.9 $\pm$ 16.1	0.0044
TC (mg/dL)	196.5 $\pm$ 14.6	179.9 $\pm$ 34.3	0.1460
LDL-C (mg/dL)	110.3 $\pm$ 16.6	98.0 $\pm$ 26.8	0.2982
HDL-C (mg/dL)	67.5 $\pm$ 26.7	70.5 $\pm$ 11.5	0.8477
RemL-C (mg/dL)	5.9 $\pm$ 1.3	3.0 $\pm$ 1.2	0.0148
RLP-C (mg/dL)	4.9 $\pm$ 1.4	2.8 $\pm$ 0.8	0.0694
RLP-TG (mg/dL)	19.5 $\pm$ 5.4	15.6 $\pm$ 2.7	0.2744
Sd-LDL-C (mg/dL)	30.7 $\pm$ 13.0	17.9 $\pm$ 5.6	0.1602
Oxidized LDL (U/mL)	4.9 $\pm$ 1.7	7.0 $\pm$ 5.2	0.1630
ApoA-I (mg/dL)	163.8 $\pm$ 49.1	164.0 $\pm$ 22.5	0.9930
ApoA-II (mg/dL)	44.0 $\pm$ 10.4	37.9 $\pm$ 6.0	0.3609
ApoB (mg/dL)	75.8 $\pm$ 10.2	65.8 $\pm$ 14.5	0.1865
ApoB-48 ( $\mu$ g/mL)	6.1 $\pm$ 2.6	2.6 $\pm$ 1.5	0.0957
ApoC-II (mg/dL)	3.6 $\pm$ 1.1	2.9 $\pm$ 1.1	0.3734
ApoC-III (mg/dL)	11.3 $\pm$ 3.7	9.1 $\pm$ 2.1	0.3531
ApoE (mg/dL)	5.1 $\pm$ 1.1	4.5 $\pm$ 0.9	0.4477

Values are expressed as the mean  $\pm$  SD, Welch's *t* test. High group: the peak triglyceride (TG) concentration  $\geq 150$  mg/dL, low group: peak TG concentration  $< 150$  mg/dL, BMI: body mass index, HbA<sub>1c</sub>: glycosylated hemoglobin A<sub>1c</sub>, TC: total cholesterol, RemL-C: remnant lipoprotein cholesterol measured with "MetaboLead RemL-C", RLP-C: remnant-like particle-cholesterol measured with "JIMRO II", RLP-TG: remnant-like particle-triglyceride, Sd-LDL-C: small, dense-LDL-cholesterol, Apo: apolipoprotein.

especially from 1 to 4 hours. In contrast, although sd-LDL-C concentrations were significantly higher in the high TG group, they gradually decreased after loading. There were no significant differences in serum concentrations of TC, LDL-C, HDL-C, and other apolipoproteins. Concentrations of glucose, insulin, and oxidized LDL also did not alter (data not shown).

### Analysis of Lipid by Electrophoretogram

Fig. 2 demonstrates representative cases of densitometric scanning patterns of electrophoretogram and lipid data before and after loading the test meal in the high and low TG groups. Sample A belongs to the high TG group. Fractions of chylomicrons and VLDL

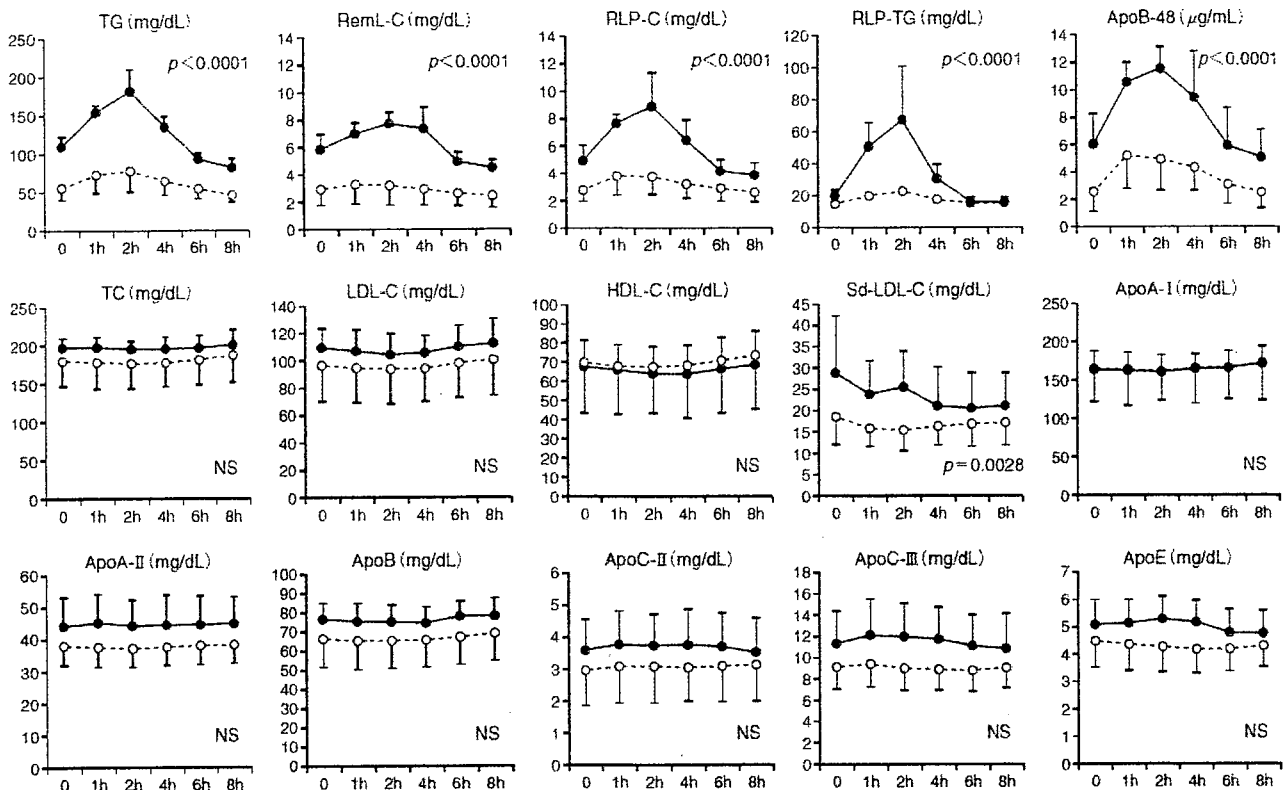


Fig. 1.

Changes in the levels of glucose and lipid parameters in subjects with <150 mg/dL (low TG group) and >150 mg/dL triglyceride concentration (high TG group) before and after loading the test meal. Responses to the test meal were compared by analysis of variance (ANOVA) for repeated measures. Open circle and broken line: low TG group, closed circle and black line: high TG group, TG: triglyceride, RemL-C: remnant lipoprotein cholesterol measured with "MetaboLead RemL-C", RLP-C: remnant-like particle-cholesterol measured with "JIMRO II", RLP-TG: remnant-like particle-triglyceride, TC: total cholesterol, HDL-C: high-density lipoprotein-cholesterol, LDL-C: low-density lipoprotein-cholesterol, sd-LDL-C: small, dense-LDL-cholesterol.

increased 1 hour after loading, peaked at 2 hours, and gradually decreased. Sample B belongs to the low TG group. We observed a slight increase of the chylomicron fraction 2 hours after loading. Thus, the peak values of TG and lipoprotein profiles in the postprandial period were different between the two cases, although fasting TG concentrations in both cases were around 80 mg/dL.

Fig. 3 shows the changes in TG concentrations of chylomicrons and VLDL, and the ratios of cholesterol to TG in HDL and LDL before and after loading the test meal. In the left panel of sample A, the higher the TG concentrations of chylomicrons and VLDL, the lower the ratios of cholesterol to TG in HDL and LDL decreased to levels around the mean-2SD of normal subjects (1.8, 2.3, respectively), as previously reported<sup>21)</sup>. In the right panel of sample B, TG contents of chylomicrons and VLDL did not increase, and the ratios of cholesterol to TG in HDL and LDL

decreased slightly.

## Discussion

In this study we analyzed serum lipids and apolipoproteins in fasting and postprandial periods among 24 young normolipidemic subjects. When we divided subjects into two groups according to the peak values of TG after loading, we found that the high TG group showed higher concentrations of TG, RemL-C, RLP-C, RLP-TG, and apoB-48 in the fasting period, although some parameters did not show significant differences. These concentrations were obviously elevated after loading in the high TG groups.

It is clear that an increase in chylomicrons and their remnants derived from the intestine is observed in the postprandial period; however, some investigators have reported that VLDL and their remnants derived from the liver are also increased, and it is

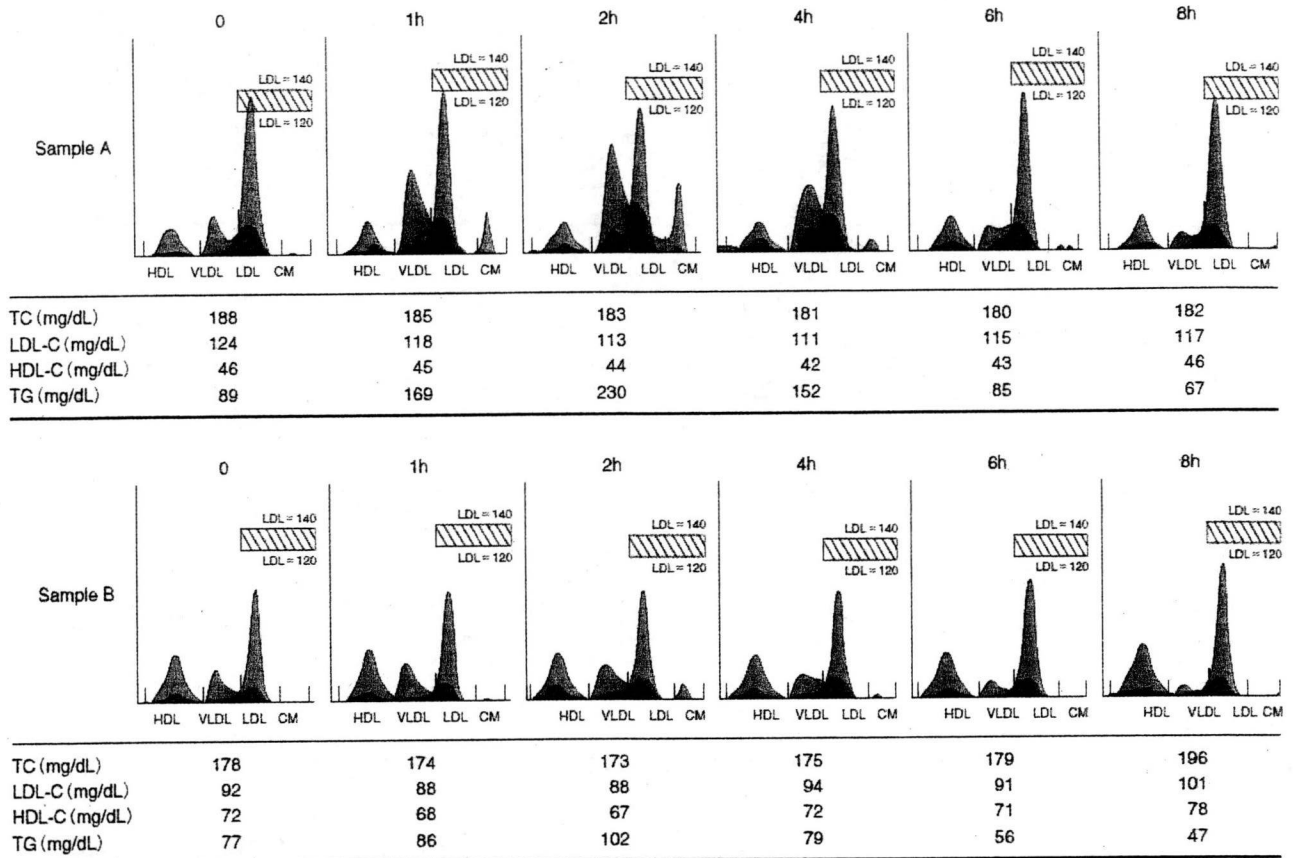


Fig. 2. Densitometric scanning electrophoretogram patterns of samples before and after loading the test meal. Elution profiles were analyzed by an automatic densitometer, Chol/Trig Combo™.

Sample A: Representative elution profile in the group with >150 mg/dL triglyceride (TG) concentration elevation after loading the test meal. Sample B: Representative elution profile in the group with <150 mg/dL TG concentration elevation before and after loading the test meal. HDL: high-density lipoproteins, VLDL: very-low-density lipoproteins, LDL: low-density lipoproteins, CM: chylomicrons, TG: triglyceride, red area: cholesterol, blue-colored area: TG.

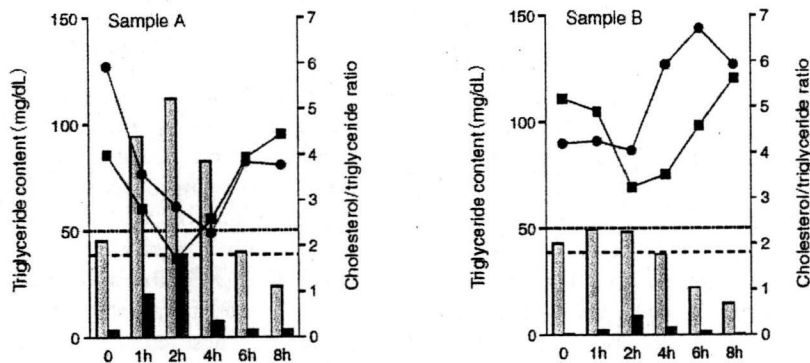


Fig. 3.

Changes in triglyceride (TG) levels of very-low-density lipoproteins (VLDL) and chylomicrons, and the ratios of cholesterol to TG of high-density lipoproteins (HDL) and low-density lipoproteins (LDL) before and after loading the test meal. Open column: TG content of VLDL, closed column: TG content of chylomicrons, closed circle: ratios of cholesterol to TG of HDL, closed square: ratio of cholesterol to TG of LDL, dashed line: ratio of cholesterol to TG of HDL of the mean-2SD in control subjects, dotted line: ratio of cholesterol to TG of LDL of the mean-2SD in control subjects.

controversial which is predominant in exogenous and endogenous lipids in the postprandial period<sup>6, 22, 23</sup>). Although the detailed mechanism remains unknown, the postprandial increase in VLDL and their remnants may be caused by reduced clearance, which was a result of competition by chylomicrons for the removal of triglycerides by lipoprotein lipase, or increased hepatic secretion of VLDL<sup>22</sup>). Receptor-mediated mechanisms are the predominant pathway by which chylomicron remnants are taken up by hepatocytes, and the LDL receptor pathway is thought to be the major mechanism for the uptake of both remnants with apoE as a ligand<sup>12, 24, 25</sup>). Impairment of or competition for the removal of both remnants in the liver may also potentially induce an increased retention time of these lipoproteins in the blood circulation. Thus, both remnant concentrations may be elevated in the postprandial period. In this study there was a remarkable elevation of apoB-48, which is a component of chylomicrons and chylomicron remnants, corroborating that lipoproteins derived from the intestine increase in the postprandial period, especially from 1 to 4 hours. ApoB concentrations (most derived from the liver) did not alter remarkably, suggesting that the postprandial increase in VLDL and their remnants may be small in young normolipidemic subjects.

Data of sample A (high TG group) demonstrated that delayed clearance of TG-rich lipoproteins in the postprandial period may be detected even in normolipidemic subjects. Impaired removal of TG-rich lipoproteins may induce the change of cholesterol and TG composition in LDL and HDL via the mechanism by which cholesteryl ester transfer protein is mediated<sup>26, 27</sup>); the higher the TG concentrations of chylomicrons and VLDL, the lower the ratios of cholesterol to TG of HDL and LDL. Thus, our data suggest that it may be possible to characterize lipid profiles conveniently in the fasting period by measuring TG, RemL-C, RLP-C, RLP-TG, and apoB-48 concentrations to detect postprandial hyperlipidemic subjects.

In the postprandial period, the elevation of RemL-C concentration did not reach a significant level, although the elevation period of RemL-C is similar to those of TG, RLP-C, and RLP-TG. These results may be due to the different measuring methods. RLP-C and RLP-TG were measured by the immune adsorption method<sup>17</sup>), while RemL-C is measured by a newly developed and convenient assay for remnant lipoproteins<sup>18</sup>). This assay utilizes surfactant and phospholipase-D to directly solubilize and degrade remnants. As such, it can be performed with an automated clinical analyzer in a short time<sup>18</sup>). There was reportedly a strong correlation between RemL-C and

RLP-C concentrations in patients with coronary artery disease<sup>28</sup>); however, our results (Table 1) suggest that differences in sensitivity for exogenous and endogenous lipoproteins between both methods may exist. The method for RLP-C and RLP-TG may be more sensitive to exogenous remnants, while RemL-C may be suitable for endogenous remnants. This hypothesis is compatible with previous reports<sup>18, 28</sup>). When we compared the two groups, the different character between RLP-C and RemL-C became clear (Table 2 and Fig. 1). The high TG group had significantly higher fasting TG and RemL-C concentrations. After loading, RLP-C, RLP-TG, and apoB-48 also became significant parameters. It can be deduced that, in the fasting period, exogenous remnants in postprandial hyperlipidemic subjects may decrease to a similar level to that in normal subjects, and endogenous remnants may remain at a significantly higher level.

There are some limitations of the present study as follows: as the study was performed with a small number of normal young subjects, only 4 individuals had the peak value of TG over 150 mg/dL as the high group. We need further examination with a larger number of normal and hyperlipidemic subjects in order to verify the TG value of 150 mg/dL, to identify the most dangerous lipid profile(s) involving remnants, apoB-48, and other parameters, and to clarify the significant differences between RLP-C and RemL-C. In addition, analyses of apoCs in remnant lipoproteins and LPL are necessary because these enzyme and proteins interfere with the apoE-mediated uptake of remnants and lipolysis<sup>29, 30</sup>). Here, since we did not examine LPL activity and protein mass measurement, we could not determine whether subjects in the high TG group have heterozygous LPL deficiency<sup>31</sup>). Of note, fasting sd-LDL-C concentration was higher in the high TG group. Interestingly, sd-LDL-C concentrations gradually decreased after loading. Here, we have no data to explain why sd-LDL-C in the high TG group but not in the low TG group gradually decreased after loading. Recently, Ogita *et al.* have reported that serum sd-LDL-C concentrations decreased after the 75 g oral glucose tolerance test and suggested that insulin can be a key modulator of sd-LDL-C concentrations<sup>32</sup>).

In conclusion, TG, RLP-C, RLP-TG, RemL-C, and apoB-48 concentrations in the fasting period may be suitable to detect and characterize postprandial hyperlipidemia in normolipidemic subjects. In future, it is necessary to reveal which parameter or combination is useful to identify postprandial hyperlipidemia with a large-scale study.